



The impact of climate model sea surface temperature biases on tropical cyclone simulations

Wei-Ching Hsu¹ · Christina M. Patricola² · Ping Chang^{1,3,4}

Received: 5 June 2018 / Accepted: 5 December 2018 / Published online: 11 December 2018
© Springer-Verlag GmbH Germany, part of Springer Nature 2018

Abstract

Sea surface temperature (SST) patterns both local to and remote from tropical cyclone (TC) development regions are important drivers of the variability of TC activity. Therefore, reliable simulations and predictions of TC activity depend on a realistic representation of tropical SST. Nevertheless, severe SST biases are common to the current generation of global climate models, especially in the tropical Pacific and Atlantic. These biases are strongly positive in the southeastern tropical basins, and negative, but weaker, in the northwestern tropical basins. To investigate the impact of the tropical SST biases on simulated TC activity, an atmospheric-only tropical channel model was used to conduct several sets of ensemble simulations. The simulations suggest an underrepresentation in Atlantic TC activity caused by the Atlantic cold bias alone, and an overrepresentation in Eastern North Pacific (ENP) TC activity due to the Atlantic cold bias and Pacific warm bias jointly. While the local impact of SST biases on TC activity is generally induced by the local anomalous SST and the associated changes in atmospheric conditions, the remote impact of the Atlantic bias on the ENP TCs is strongly driven by the change in topographically forced regional circulation. Moreover, an eastward shift in Western North Pacific TCs was generated by the Pacific SST biases, even though basin-wide TC activity indicators change insignificantly. The results indicate the importance of considering SST bias effects on simulated TC activity in climate model studies and highlight key regions where reducing SST biases could potentially improve TC representation in climate models.

Keywords SST bias · Tropical cyclones · Tropical channel model · Climate model bias

1 Introduction and background

Tropical cyclones (TCs) are one of the most destructive natural hazards, with hurricanes Katrina (2005), Sandy (2012), and Harvey, Irma, and Maria (2017) among the most damaging and deadliest natural disasters in the U.S. (Blake et al. 2007, 2013; Emanuel 2017; Shuckburgh et al. 2017; Klotzbach et al. 2018). Therefore, in order to reduce loss of life

and mitigate economic losses, improving TC prediction on weather to climate timescales is a high priority research area.

Sea-surface temperature (SST) variability in both local and remote basins provides one major source of seasonal to multidecadal TC predictability. For example, Atlantic and Pacific SST variability exerts a significant influence on Atlantic TCs. The El Niño-Southern Oscillation (ENSO) in the tropical Pacific and the Atlantic Multidecadal Variability (AMV) and Atlantic Meridional Mode (AMM) influence Atlantic TC activity through changes in maximum potential intensity (e.g. Emanuel 2007), vertical wind shear (e.g. Gray 1984a, b; Emanuel 2007; Vimont and Kossin 2007), low-level vorticity (e.g. Emanuel 2007; Vimont and Kossin 2007), and tropospheric moisture (e.g. Vimont and Kossin 2007). Pacific TC activity also depends on SST, with increasing tropical SST locally driving enhanced TC intensity in the eastern and western North Pacific (Webster et al. 2005). In addition, ENSO influences eastern and western North Pacific TC activity, and the AMM provides seasonal TC predictability for the eastern Pacific (Gray 1984a;

✉ Wei-Ching Hsu
wchsu@hawaii.edu

¹ Department of Oceanography, Texas A&M University, College Station, TX, USA

² Climate and Ecosystem Sciences Division, Lawrence Berkeley National Laboratory, Berkeley, CA, USA

³ Department of Atmospheric Science, Texas A&M University, College Station, TX, USA

⁴ Physical Oceanography Laboratory/Qingdao Collaborative Innovation Center of Marine Science and Technology, Ocean University of China, Qingdao, China

Whitney and Hobgood 1997; Wang and Chan 2002; Camargo and Sobel 2005; Wang et al. 2013; Jin et al. 2014; Jien et al. 2015; Patricola et al. 2017). Therefore, reliable climate model simulations of TC activity depend on a realistic representation of modes of climate variability on seasonal to multi-decadal timescales, as well as climatological mean SSTs.

However, severe SST biases exist in the tropical Pacific and Atlantic in most of the Intergovernmental Panel on Climate Change (IPCC) coupled global climate models (CGCMs) (e.g., Richter 2015). Figure 1 shows the multi-model ensemble-averaged seasonal mean (April to November) of the tropical SST biases in Atlantic and Pacific from the Coupled Model Intercomparison Project Phase 5 (CMIP-5) models (details in Methodology). The SST bias in the Indian Ocean is not shown, since its magnitude is relatively small. Very large warm biases cover the southeastern tropical Atlantic and Pacific (Wang et al. 2014), with the Atlantic bias reaching 6 °C in some models (Xu et al. 2014a, b). In addition, cold SST biases occur in the northwestern Atlantic and Pacific, albeit with weaker amplitudes. Wang et al. (2014) and Zhang et al. (2014) suggest interhemispheric links of the biases in Atlantic and Pacific.

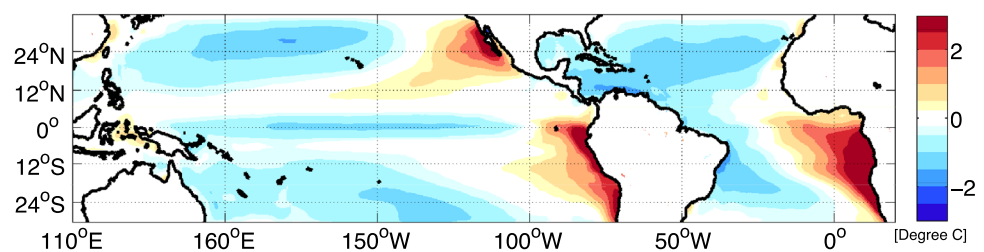
Several mechanisms have been identified to cause the SST biases, which can vary from region to region (Richter and Xie 2008; Li and Xie 2012; Patricola et al. 2012; Xu et al. 2014b). The tropical cold biases mainly originate from atmospheric errors in cloud cover (Li and Xie 2012) and trade winds (Liu et al. 2012), and can be largely reduced by increasing model resolution (Zuidema et al. 2016). The mechanisms for the warm biases in eastern Pacific and Atlantic are more complex. While the processes driving the warm bias in the Atlantic are mostly rooted in the narrow near-shore winds along the Benguela coast (Xu et al. 2014a, b; Small et al. 2015; Patricola et al. 2016), errors in marine stratocumulus and associated short wave radiation can contribute significantly to the southeastern Pacific warm bias (Masunaga et al. 2002; Painemal and Minnis 2012; Zuidema et al. 2016), even though the patterns of the biases are similar in the two ocean basins. Moreover, nonlinear processes associated with ocean mesoscale eddies may contribute to the warm biases in the eastern ocean basins (Toniazzi et al. 2010; Colas et al. 2012). Atlantic equatorial westerly wind

biases can also remotely influence the eastern warm SST biases through oceanic Kelvin waves (Richter 2015).

Even though the mechanisms that cause the SST biases have been widely studied, the impact of the biases on TC simulations and seasonal predictions has not been fully understood. Dynamical climate models are now utilized to make experimental seasonal TC predictions, owing to model developments and improvements in computational capabilities (e.g., Wang and Lee 2009; LaRow et al. 2010; Murakami et al. 2016; Zhang et al. 2017). One forecasting approach is based on atmosphere-only models with predicted SSTs as a boundary condition. For this approach, important aspects of TC-ocean interactions (e.g., Lin et al. 2013) are not represented. Another seasonal TC forecast approach uses coupled atmosphere–ocean models. However, the severity of the tropical SST biases can potentially have considerable impacts on TC simulations and predictions. Vecchi et al. (2014) show improvements in simulated TC genesis and track by reducing SST biases in a high-resolution CGCM simulation through adjusting momentum, enthalpy, and freshwater fluxes. They suggest that the improved TC representations are likely achieved by improvements in simulated large-scale climatological conditions and interannual variability. Zhao et al. (2010) emphasized the importance of SSTs on seasonal TC forecasts by comparing forecasts using persisted and observed SST anomalies in a high-resolution (50 km) atmospheric-only model. The results potentially indicate that TC forecast skill depends strongly on the ability of the models to predict the relative change of SST in the TC main development region (MDR) to tropical mean SST.

The SST biases can also introduce large uncertainties into future projections of TC activity based on climate models. There is no consensus on projected changes in future TC frequency, although the most recent simulations suggest a slight reduction in overall TC numbers but an increase in the percentage of intense TCs (e.g., Emanuel 2005; Holland and Webster 2007; Bender et al. 2010; Knutson et al. 2010; Camargo and Hsiang 2016). Nevertheless, projections of future TC location changes, such as TC tracks and land-fall frequency, are not robust, and sub-regional projections remain highly uncertain (Camargo and Hsiang 2016). A clear understanding of future changes in TCs requires reliable simulations of the mean and variability of SST.

Fig. 1 The April–November averaged CMIP5 multi-model mean tropical SST biases (°C)



Although future increases in computing power and model resolution may partially alleviate SST bias problem, it is likely to persist in models to some degree for at least a decade or longer, as model representation of atmospheric and oceanic processes also contributes to the SST biases (Richter 2015). Therefore, it is crucial for us to take into account the impact of these biases on simulations of TCs activity. Here we addressed the question: How do Atlantic and Pacific SST biases impact the simulated TC climatology? By conducting suites of model simulations, we improved our understanding of how the warm and cold SST biases individually influence simulated TC activity, and through what mechanisms. Moreover, we also considered how the Atlantic and Pacific SST biases jointly influence TC simulations and assessed their relative importance in affecting TC simulations in different regions, as modes of tropical Pacific and Atlantic variability are known to exert joint influences on Atlantic TC activity (Patricola et al. 2014). By splitting the biases up by region and by sign, we identified which biases are most detrimental to TC simulations and what impact to consider for basin-wide TC activity. Moreover, while keeping in mind that remote relationships occur between the biases in different ocean basins, we also addressed the question: how do remote impacts of SST biases from basins outside of the region of interest impact TC activity? Although previous studies have shown that SST biases can impact TC simulations, the impact has not been systematically quantified and the pathways by which the biases influence TCs have not been understood. The objective of this study is to gain insight into the impact of the SST biases on TC simulations at seasonal-to-interannual timescales. More importantly, we will shed light on the underlying dynamics of the SST biases' impact on TC simulations.

The sections in this chapter are organized as follows. Section 2 describes the modeling tool and experiment design. Section 3 presents the results of the model experiments where SST biases are specified either individually or jointly in different tropical ocean basins. Section 4 discusses the implications of the results and summarizes the main conclusions.

2 Research methods—model description and experimental designs

2.1 Model description

We utilized a Tropical Channel Model (TCM) configuration (Patricola et al. 2016, 2017) of the Weather Research and Forecasting (WRF) Model (Skamarock et al. 2008) developed by the National Center for Atmospheric Research (NCAR). This model is more suitable for this study compared to many global climate models (GCMs) due to its

non-hydrostatic dynamical core and finer resolution. The TCM extends around the global tropics from 30°S to 50°N, and has 27 km TC-permitting horizontal resolution and 32 levels in the vertical. While the horizontal resolution of the TCM is too coarse to resolve the details of the individual TCs, it is sufficient to investigate the statistics of TC activity (Patricola et al. 2016). By setting the model domain to the global tropics, we allow atmospheric responses to SST forcings to propagate around the globe in the tropics and subtropics. Moreover, by setting the northern boundary at 50°N, atmospheric teleconnections that affect the MDR from outside the tropics can be considered, as teleconnections between different tropical ocean basins can be linked through regions outside of the tropics (Nobre and Shukla 1996).

The sensitivity of physical parameterizations of the WRF model was well tested over the Atlantic MDR (Patricola et al. 2014), and the TCM was tested over both the Atlantic and Pacific basins (Patricola et al. 2016, 2017). However, we note some problems with the model. For example, the TCM tends to generate too much rainfall over Africa and the Amazon, underestimate the maximum near-surface wind speed of TCs, and overestimate the number of Atlantic and ENP TCs (Patricola et al. 2016). Despite these issues, the TCM reproduces the atmospheric responses to ENSO and AMM reasonably well (Patricola et al. 2016, 2017). Therefore, with these known problems, the TCM is still a suitable tool for this study.

2.2 Experimental designs

We conducted extensive WRF TCM experiments forced by surface boundary conditions with and without climatological 6-hourly SST biases. By prescribing the SST forcings to the TCM, we can isolate the atmospheric response to specific regions of SST bias, which is important as different mechanisms generate the SST biases in different regions. The SST biases were calculated from the CMIP-5 (Taylor et al. 2012) multi-model (37 models) ensemble mean subtracted from the National Oceanic and Atmospheric Administration (NOAA) Optimum Interpolation (–OI) observed SST (Reynolds et al. 2007) covering the period of 1984 to 2004, and were then interpolated to 6-hourly from monthly, and to the 27 km grid of the TCM. A suite of simulations (Table 1) were conducted to quantify individual and joint effects of SST biases on TC activity by separating the Atlantic and Pacific SST biases into warm, cold, and total (combining warm and cold) biases. The biases near the lateral boundaries were smoothed over 5 degrees in the latitudinal direction. Even though the amplitudes of seasonal variation of the biases are smaller than the biases themselves (Wang et al. 2014), we included the annual cycle of the SST biases in our simulations.

Table 1 Experiment names for control and bias runs, and the associated SST biases that included in the SST forcings for each experiment

SST bias	Experiment name
Control (without bias)	<i>CTRL</i>
Atlantic warm bias	<i>AtlWB</i>
Atlantic cold bias	<i>AtlCB</i>
Atlantic total bias	<i>AtlTB</i>
Pacific warm bias	<i>PacWB</i>
Pacific cold bias	<i>PacCB</i>
Pacific total bias	<i>PacTB</i>
Atlantic and Pacific total bias	<i>AtlPacTB</i>

The biases were added to the control SST to produce the warm, cold, and total bias simulations. Figure 1 shows the seasonal mean (from April to November, to focus on the TC season) of the climatological 6-hourly SST biases that we used in the experiments. While the SST biases were calculated based on the 1984–2004 NOAA-OI SST and CMIP5 simulations, the control SST was based on the monthly 1950–2014 climatology from the Hadley Center Global Sea Ice and Sea Surface Temperature dataset (HadISST) (Rayner et al. 2003). HadISST was utilized for the control SST because the product covers a longer time period, whereas the NOAA-OI SST was used to calculate SST biases because the resolution is finer. We do not expect details between HadISST and NOAA-OI SST to significantly impact the results of this study, as the SST biases have much larger amplitude than the difference between the two SST products.

To quantify the impact of SST biases, the ensemble of control simulations (*CTRL*) serves as a reference for experiments including the Atlantic warm bias (*AtlWB*), Atlantic cold bias (*AtlCB*), Atlantic total bias (*AtlTB*), Pacific warm bias (*PacWB*), Pacific cold bias (*PacCB*), Pacific total bias (*PacTB*), and the combined Atlantic and Pacific total bias (*AtlPacTB*) simulations (Table 1). The warm and cold biases are defined at every grid point with SST bias values greater and less than zero, respectively. Initial conditions (ICs) and lateral boundary conditions (LBCs) were provided by the 6-hourly NCEP-U.S. Department of Energy (DOE) Atmospheric Model Intercomparison Project II (AMIP-II) Reanalysis (NCEP-2) from the years 1989 and 1996 (Kanamitsu et al. 2002). The 2 years were chosen for LBCs since climate modes such as ENSO during the simulation period of April to November were in neutral phases, in order to avoid a strong influence of the climate modes through the northern mid-latitude LBCs (Patricola et al. 2016). To focus on the TC season in the northern hemisphere, the simulations were started in April and ended in November. The first 2 months were discarded as spin up, with analysis covering June to the end of November. An ensemble of 16 runs was generated by altering the start date to generate different ICs for each

ensemble member of each experiment in order to quantify the statistical significance of the results.

2.3 Quantifying TC activity

The tracking algorithm from Walsh (1997) was used to identify simulated TCs, including tropical storms and hurricanes or typhoons (depending on the ocean region). To be identified as a tropical cyclone, the system must generate south of 30°N, last at least 2 days, and have a warm core. Moreover, an identified TC must have a closed surface pressure minimum, a minimum 10-m wind speed of 17.5 ms⁻¹, and satisfy a 850-hPa vorticity threshold over its center. The resolution used to calculate the track density is 2° longitude by 2° latitude. A comparison between the track density from the Revised Atlantic Hurricane Database (HURDAT2) (Landsea et al. 2015) and from TCM ensemble of the climatology simulation in the ENP and Atlantic is shown in Supplementary Fig. 6 in Patricola et al. (2016).

To investigate the impact of SST biases on TC activity, we calculated the simulated accumulated cyclone energy (ACE), which accounts for TC strength, number, and duration (Bell et al. 2000). ACE is the summation of the square of the 6-hourly maximum sustained wind speed of TCs over a TC season. Furthermore, to understand the underlying dynamics linking SST biases to TC simulations, we examine the Genesis Potential Index (GPI) (Emanuel and Nolan 2004). By calculating GPI, we can quantitatively estimate how various environmental variables influence changes in TC activity:

$$GPI = \left| 10^5 \eta \right|^{\frac{3}{2}} \left(\frac{H}{50} \right)^3 \left(\frac{V_{pot}}{70} \right)^3 (1 + 0.1 V_{shear})^{-2}.$$

The GPI is calculated from the monthly mean of absolute vorticity at 850 hPa (η), relative humidity at 600 hPa (H), potential intensity (V_{pot}), and vertical wind shear between 850 and 200 hPa (V_{shear}). The potential intensity (PI) is computed based on atmospheric (temperature and specific humidity) vertical profiles, sea level pressure, and SST. While GPI does not explain all variability associated with TCs, it is a suitable index for investigating the conditions that influence the TC activity (Camargo et al. 2007; Patricola et al. 2014).

3 Results

3.1 Atlantic SST biases

To quantify the impact of Atlantic SST biases on TC spatial variability in Atlantic and Pacific basins, we computed the spatial differences in the TC track densities between

the Atlantic bias and the control simulations (Fig. 2). The Atlantic warm bias produced no significant impact on TC track density (Fig. 2a) and genesis locations (not shown). However, the Atlantic cold bias caused a marked decrease in Atlantic TC track density, and a remote increase in ENP TC track density (Fig. 2b), with an insignificant change in Atlantic genesis density and a positive genesis density anomaly near the coast of the ENP (not shown). Note that the region of positive anomaly in track density in the ENP is slightly offshore, and the magnitude of the anomaly is even larger than that in the Atlantic. Combing both cold and warm biases in the Atlantic, the bias (*AtITB*) impacts the track density in a similar way as *AtICB*, but with smaller magnitudes (Fig. 2c). Moreover, the Atlantic SST biases produced no statistically coherent response in WNP track density.

Other than the impact on spatial patterns of TCs, we also investigated the basin-wide TC variability by calculating ACE and the number of TCs, and the values in different ocean basins computed from the control simulation and the Atlantic bias experiments are shown (Fig. 3; Table 2). Both *AtICB* and *AtITB* generate lower ensemble median (Fig. 3) and mean (Table 2) values of ACE and TC numbers in the Atlantic and higher values in ENP compared to *CTRL*. These changes generated by *AtICB* and *AtITB* are all significant at the 5% level (two-sample student t-test). Besides, both *AtICB* and *AtITB* generate a decrease in Atlantic TC intensities (not shown), corresponding to the smaller ACE values, and an increase in ENP TC intensities that co-occurs with larger ACE values. Moreover, similar to the impact on track density, the impact of Atlantic cold and total biases on ACE

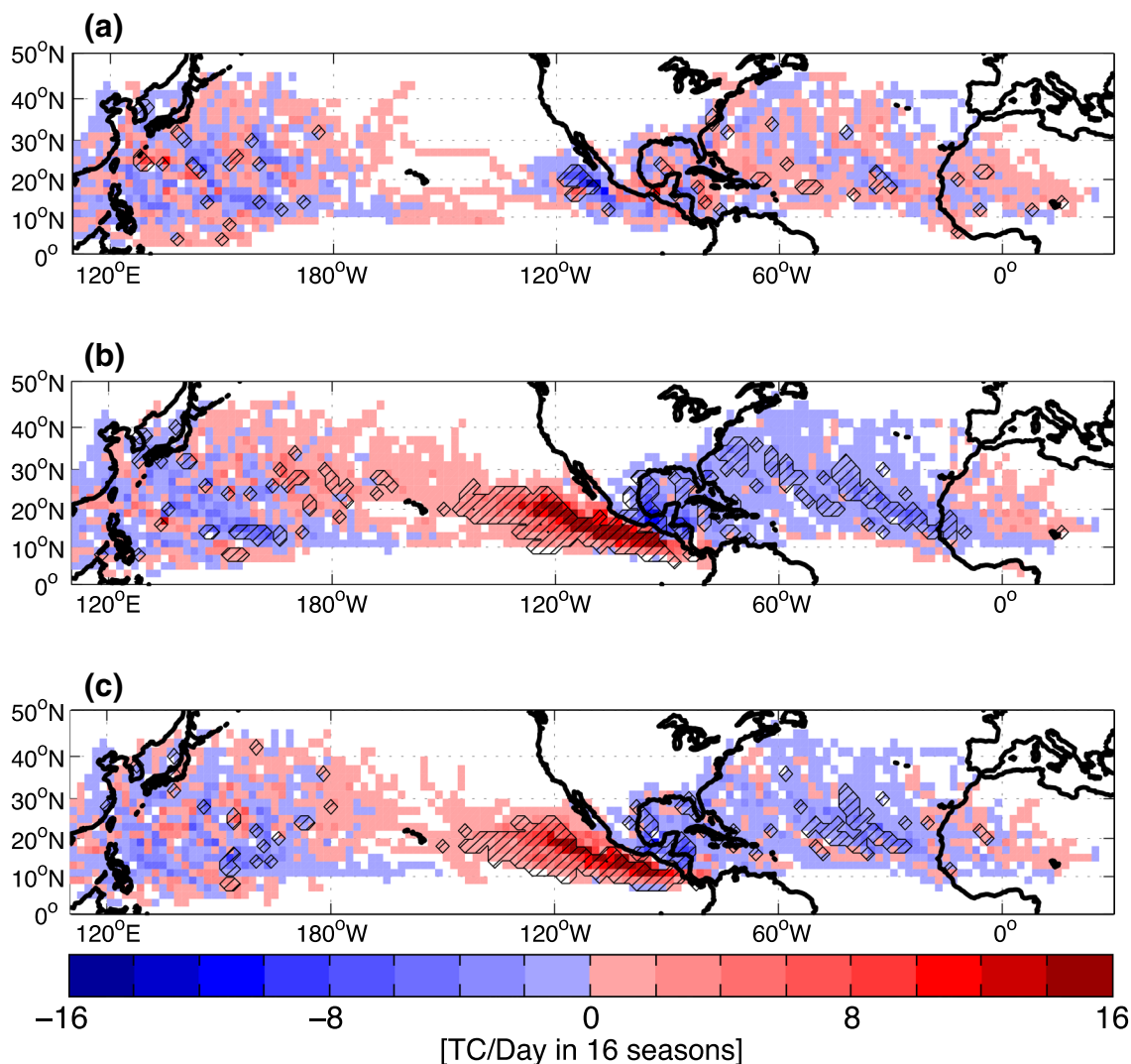


Fig. 2 The differences between track density ensemble means of **a** Atlantic warm bias (*AtIWB*) and control (*CTRL*) runs, **b** Atlantic cold bias (*AtICB*) and control (*CTRL*) runs, and **c** Atlantic total bias

(*AtITB*) and control (*CTRL*) runs. Hatched regions passed the two-sample student t-test at 5% significance level

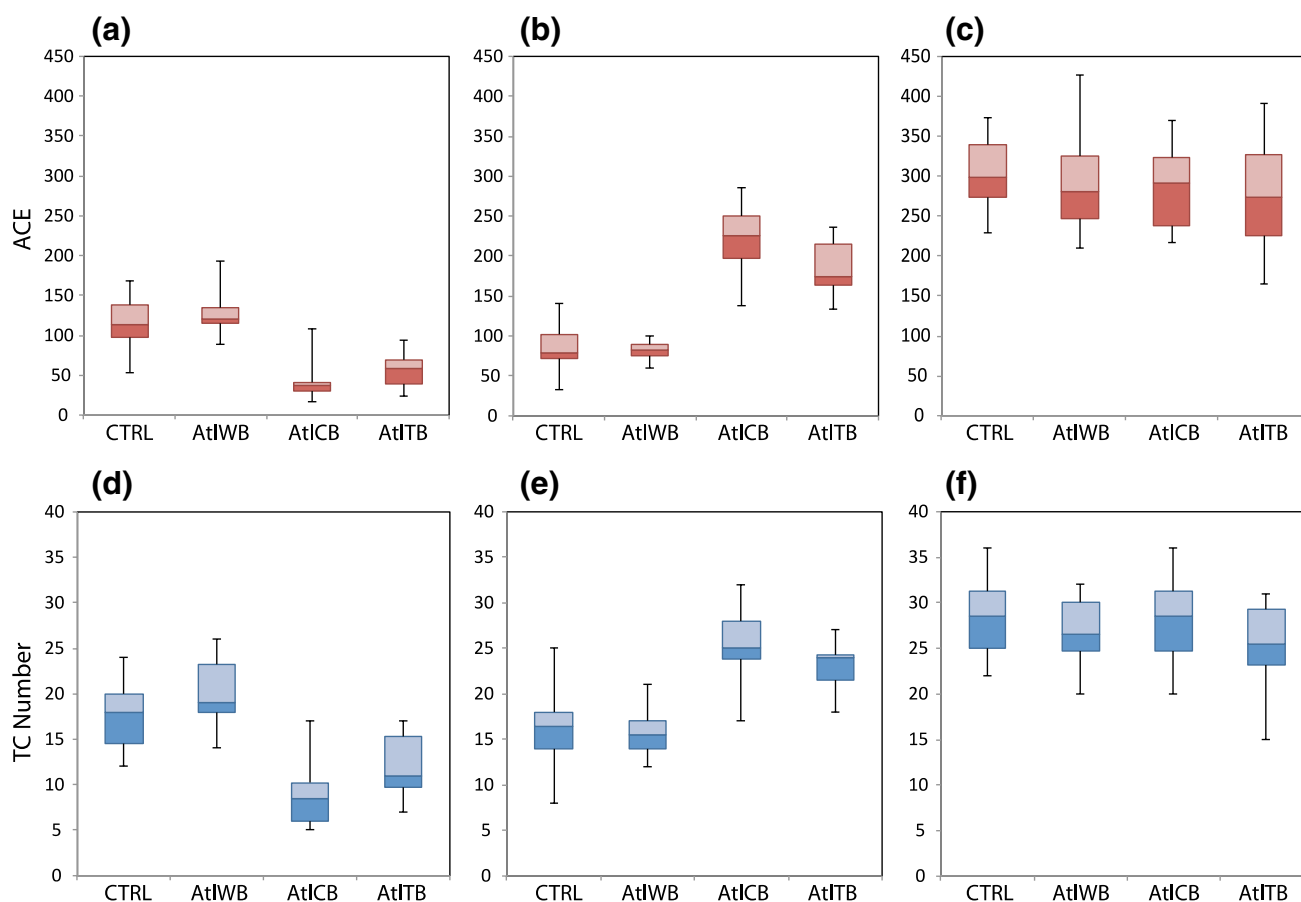


Fig. 3 Boxplot of simulated Accumulated Cyclone Energy (ACE) (a to c) and number of TCs (d to f) from control (*CTRL*), Atlantic warm (*AtlWB*), cold (*AtlCB*), and total (*AtlTB*) bias runs (16 ensemble members each) in Atlantic (a and d), eastern North Pacific (b and e), and western North Pacific (c and f) basins. The horizontal line

between light and dark shading represents the median of the ensemble values, while the upper boundary of the light color box represents the 75 percentile and the lower boundary of the dark color box represents the 25 percentile. The whiskers show the maximum and minimum ensemble values

Table 2 Ensemble means (from 16 ensemble members each) of ACE and the number of TCs from control (*CTRL*) and Atlantic bias (*AtlWB*, *AtlCB*, and *AtlTB*) runs in both real number and percentage difference from *CTRL* (only shown if the difference from *CTRL* is significant at the 5% level)

	<i>CTRL</i>	<i>AtlWB</i>	<i>AtlCB</i>	<i>AtlTB</i>
Atlantic ACE	116	128	42 [− 64%]	57 [− 51%]
ENP ACE	87	81	220 [153%]	185 [113%]
WNP ACE	302	295	285	278
Atlantic number of TCs	18	20	9 [− 50%]	12 [− 33%]
ENP number of TCs	16	16	26 [63%]	23 [44%]
WNP number of TCs	28	27	28	25

and TC number is stronger in the ENP basin (remotely) than in the Atlantic basin (locally) (Table 2). On the other hand, based on values in ACE and TC numbers, the Atlantic warm bias does not significantly (5% level) impact TCs in any of the tropical ocean basins, and all the Atlantic SST biases

insignificantly influence WNP TCs. Note that even if we consider the internal variability (or the range of the values of the ensemble members), the values of ACE and number of TCs generated by *AtlCB* and *AtlTB* in the Atlantic and ENP are considerably different from those of *CTRL* (Fig. 3).

In addition, to understand the underlying dynamics linking SST biases to TC simulations, we examined the GPI (Fig. 4) and the associated atmospheric variables (not shown). The patterns of significant GPI changes are consistent with the changes in ACE and the number of TCs. The cold (Fig. 4b) and total (Fig. 4c) SST bias forcings induce a decrease in ensemble-mean GPI in the Atlantic MDR and Gulf of Mexico (GoM), and an increase in the ENP. The Atlantic warm bias alone insignificantly impacts GPI (Fig. 4a). Therefore, we focus on *AtlCB* and *AtlTB* to investigate the dominant GPI terms (atmospheric variables) that contribute to the GPI change driven by Atlantic SST biases. The impact of *AtlTB* is not significantly different from that of *AtlCB*, suggesting that the cold bias, rather than

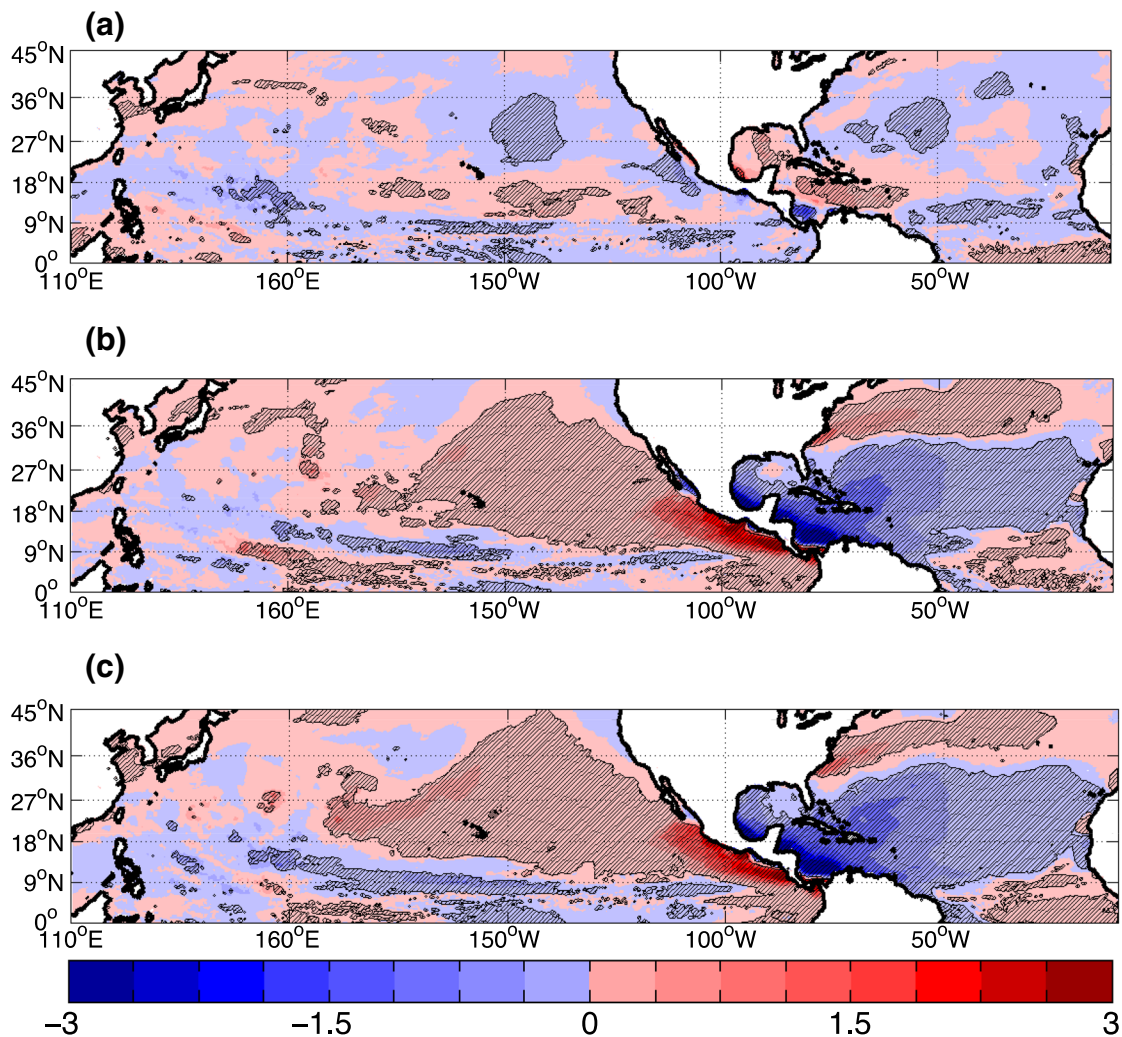


Fig. 4 The differences between GPI ensemble means of **a** Atlantic warm bias (*AtIWB*) and control (*CTRL*) runs, **b** Atlantic cold bias (*AtICB*) and control (*CTRL*) runs, and **c** Atlantic total bias (*AtITB*)

and control (*CTRL*) runs. Hatched regions passed the two-sample student t-test at 5% significance level

the gradient generated by both the cold and warm biases, mainly contributes to the anomalous GPI patterns.

GPI changes forced by Atlantic SST biases can be further diagnosed by computing contributions from environmental variables including vertical wind shear, mid-tropospheric relative humidity, potential intensity, and vorticity. To estimate the contribution from each factor, we calculated the GPI by setting one term in GPI to the value from one of the perturbed simulations, and other terms to values from the control simulation, and then compared to the *CTRL* GPI (Camargo et al. 2007; Patricola et al. 2014, 2016). Only the results for *AtICB* (Fig. 5) are shown due to the similarity between the GPI responses in the *AtICB* and *AtITB* experiments. In both the Atlantic cold and total bias runs, the mid-tropospheric humidity, vertical wind shear, and potential intensity all contribute to the decrease in Atlantic GPI, while only the shear term contributes to the increase in ENP GPI.

(The negative contribution from the humidity and vorticity terms compensates the large positive contribution from the shear term by a small magnitude along the coast of the ENP.) Moreover, the weak positive GPI anomalies in the central Pacific in *AtICB* and *AtITB* arise from the humidity term.

The response in atmospheric conditions (e.g., mid-tropospheric relative humidity and vertical wind shear) is consistent with the associated GPI term (not shown). For example, the vertical shear is enhanced by the *AtICB*, consistent with the relationship found in previous studies: with cold anomaly in northern Atlantic SST, the strengthened subtropical high can induce easterly low-level wind anomalies in the MDR, and further enhance the local vertical wind shear (Vimont and Kossin 2007). Moreover, the change in tropospheric humidity can be locally linked to the change in surface latent heat flux generated by SST anomalies in the Atlantic (Vimont and Kossin 2007). Note

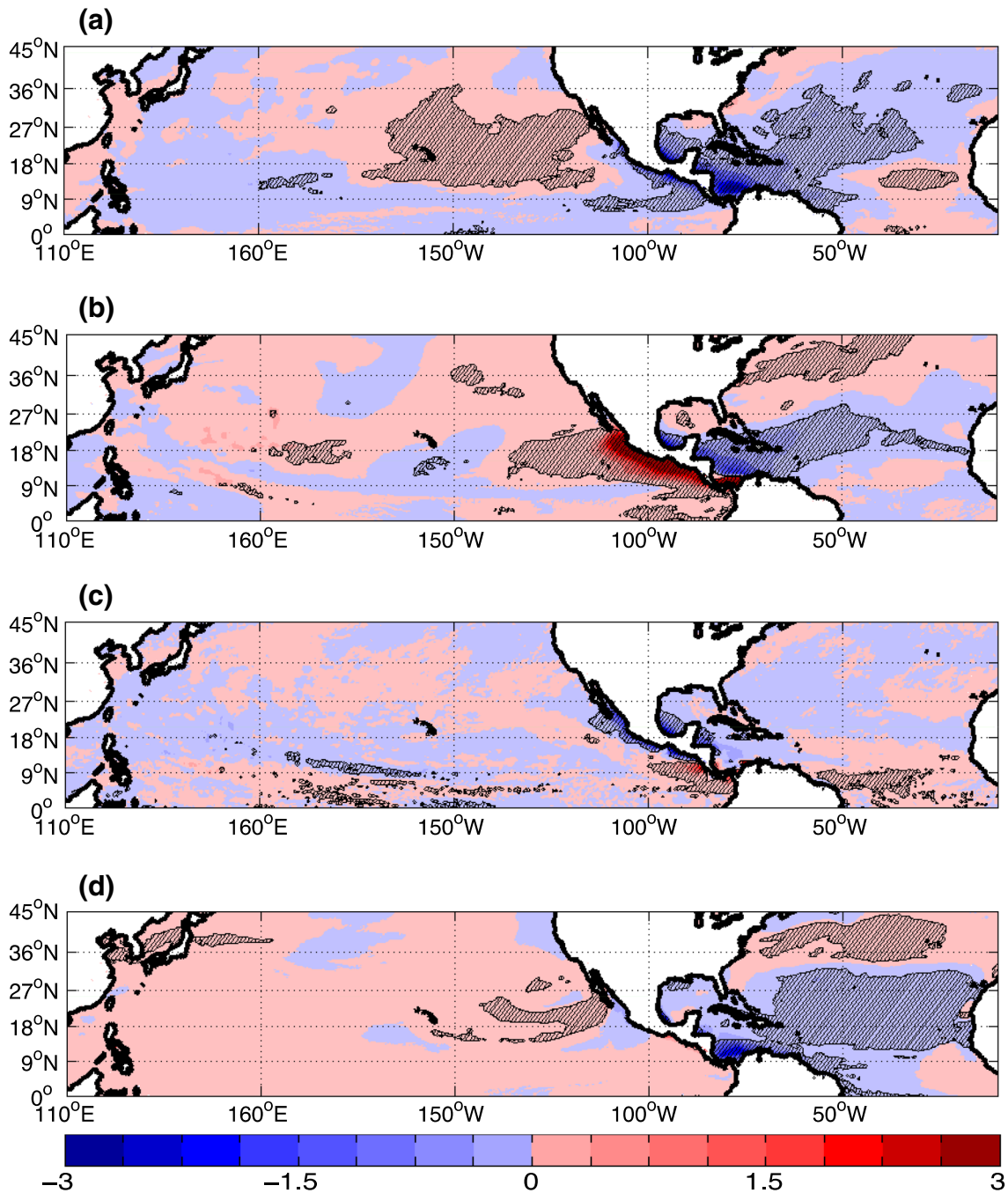


Fig. 5 The differences of ensemble mean GPI values between Atlantic cold (AtlCB) bias runs and control (CTRL) runs contributed from **a** humidity, **b** shear, **c** vorticity, and **d** potential intensity terms. Hatched regions passed the two-sample student t-test at 5% significance level

that in order to test the robustness of the results, all of the above analyses (and those for Pacific and combined Atlantic and Pacific SST bias experiments) were repeated by randomly choosing 8 out of the 16 ensemble members. There is little difference in the results, suggesting that the ensemble size is sufficiently large to generate robust findings. In particular, the ensemble means of the results from 1989 to 1996 forced members (8 members each) were

compared, and no statistically significant differences in TC activity were shown.

It has been shown that SST anomalies in the tropical Atlantic can remotely influence atmospheric circulations and SSTs in the tropical Pacific on interannual to centennial timescales (Kucharski et al. 2016). On interannual timescales, previous studies have shown that the teleconnection generated by Atlantic SST variability can impact

the Pacific basin through a Walker-type circulation response (Patricola et al. 2017; Zhang et al. 2017), consisting of near-surface wind anomalies triggered by equatorial Kelvin waves (Rodríguez-Fonseca et al. 2009; Ding et al. 2012; Polo et al. 2015), and/or Rossby wave responses (Ham et al. 2013a, b). In our *AtICB* simulations, while a Walker-type circulation response similar to the negative AMM experiment in Patricola et al. (2017) can be seen (Fig. 6a), the remote impact of Atlantic cold bias on ENP TC activity, especially the shear contribution, is also strongly influenced by the change in regional circulation inducing by the topography.

To examine the remote impact dominated by the shear term, we investigated both the *CTRL* and *AtICB* simulated wind profiles near the regions with the largest shear contribution from *AtICB* (Fig. 5b). In *CTRL* simulations (Fig. 6b), low-level easterlies, generated by trade wind and the associated Caribbean low level jet (CLLJ), appear in the Caribbean/Atlantic region with the corresponding westerlies on top around 200 hPa induced by the occurrence of the Central America mountain. On the lee-side of the Central American topography, low-level westerly flow occurs with easterly flow in upper levels. Circulations on the lee-side and in the Caribbean region (windward side) both contribute to an ascending wind on top of the Central American mountain region, generating a maximum rainfall region in the TCM (not shown). Moreover, in the western part of the ENP, a circulation cell (or double cell, as it is generated by both the Hadley Cell and Walker circulation) exists, with low-level easterly winds occurring with upper-level westerlies. A descent motion band around 130°W is then generated by

the double cell and the lee-side circulation. Note that since the orography of the region is highly complex, and the peaks of the mountains are at different altitudes depending on the location (both longitude and latitude), the winds can flow through the mountain gaps in some locations, but in most places are forced to ascend on the windward side of the mountain due to rising orography (Fig. 6).

In the *AtICB* simulations (Fig. 6c), stronger low-level easterly flow occurs in the Caribbean/Atlantic region with enhanced upper-level westerlies. This strengthening of the circulation on the windward side of the mountain is contributed by strengthening of the CLLJ. The strength of the CLLJ is correlated to the SST difference between the tropical Atlantic and ENP, and is also strongly controlled by the land-sea temperature difference between the Caribbean and the northern part of the southern America land (e.g., Whyte et al. 2008). With the Atlantic cold bias, the pressure gradient is enhanced between the ocean basins and between the land and sea, and therefore the CLLJ is strengthened. However, since the air coming from the Atlantic/Caribbean region is colder and dryer (due to the Atlantic cold SST bias) compared to *CTRL*, the latent heat release associated with the orographic lifting is weaker than that in *CTRL*. This leads to a weakened ascending motion in *AtICB* than in *CTRL*, resulting in an anomalous descending wind over the mountain and the windward region.

Figure 7 shows rainfall and vertical-integrated moisture convergence differences between *AtICB* and *CTRL*. A decrease in regional rainfall over Central America is indicative of a weakening in the diabatic heating, while a decrease

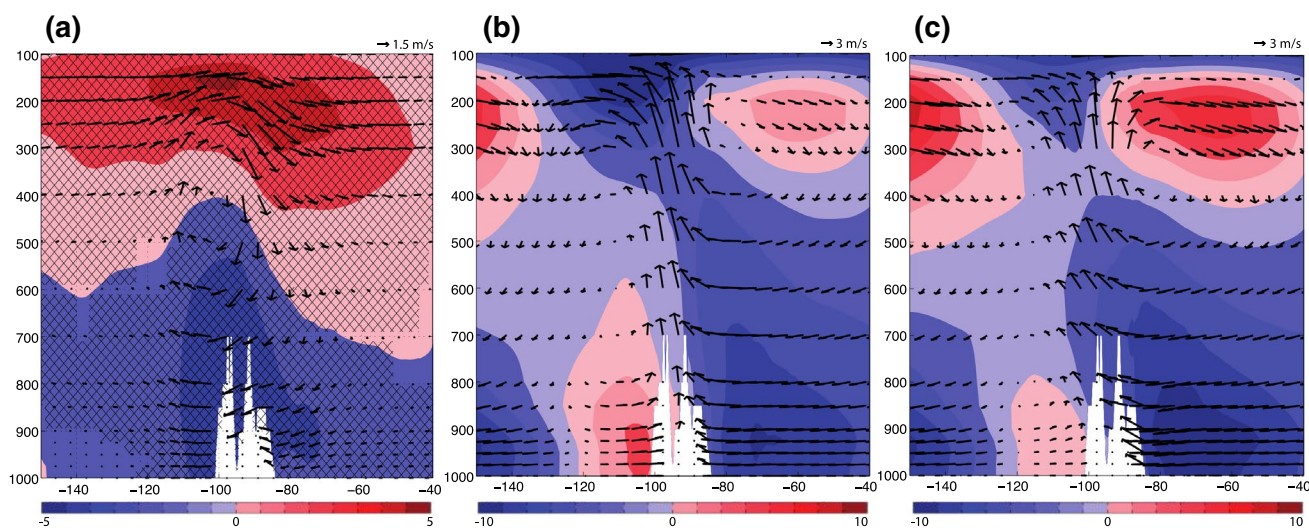


Fig. 6 The wind cross-section (degree longitude vs. hPa) along 15°N (averaged from 12.5°N to 17.5°N), where the *AtICB* shear contribution (to GPI anomaly) and cold bias induced zonal wind anomalies at 200 hPa and 850 hPa show the largest values. **a** shows the ensemble-averaged anomalous wind profile (in arrows [m/s]) calculated from zonal (*u*) and vertical (*w*) wind (times 3000 for scaling) differ-

ences between *AtICB* and *CTRL* runs, and the zonal wind anomalies (in shaded color) (in m/s) from *AtICB* comparing to *CTRL*, while **b** shows the *CTRL* ensemble-averaged wind profile, and **c** shows the *AtICB* wind profile. Hatching region in **a** indicates the differences passing the 95% student t-test

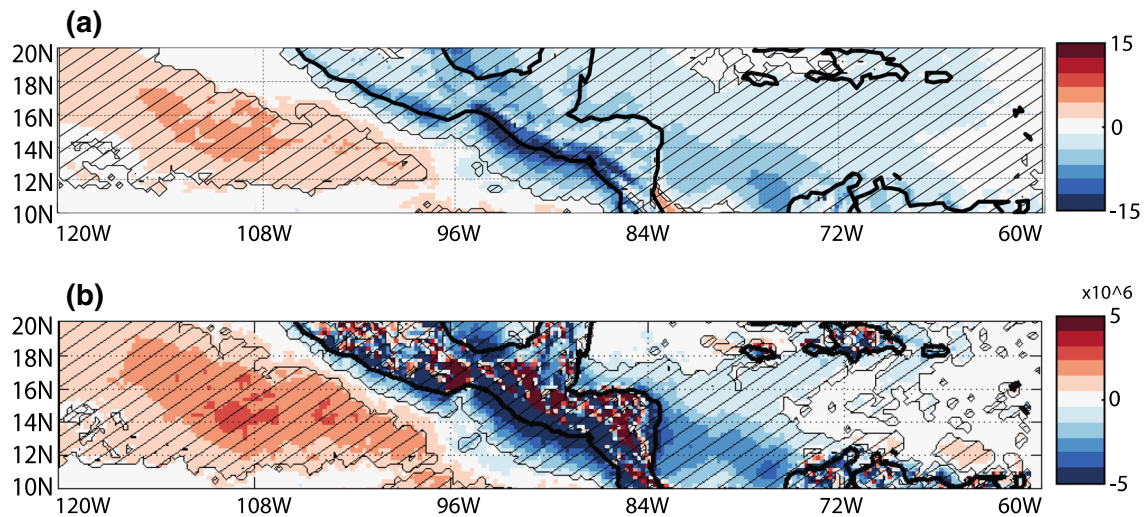


Fig. 7 Seasonal-mean precipitation **(a)** (in mm/day) and seasonal-mean vertical-integrated (1000 hPa to 500 hPa) moisture convergence **(b)** (in $\text{g/kg}\cdot\text{s}^{-1}$) differences between *AtlCB* and *CTRL*. Red colors in **a** indicate more precipitation in *AtlCB* than *CTRL*. While red colors

in **b** indicate anomalous moisture convergence, blue colors indicate anomalous moisture divergence. Hatched regions passed the two-sample student t-test at 5% significance level

in the moisture convergence from windward side to coastal leeward side of the mountain suggests a reduced moisture supply in the region. Note that due to the complexity of the terrain, the spatial pattern of moisture convergence over the mountain is messy. As a result, the cold SST bias produces a clockwise anomalous vertical circulation above the mountainous region in the Central America (Fig. 6a), which acts to strengthen the circulation over the Caribbean and Atlantic and weaken the circulation over the far eastern ENP (Fig. 6b). As such, the vertical wind shear is strengthened over the Caribbean and Atlantic and reduced over the Caribbean and Atlantic sector. This offers an explanation for the sharp change in sign of vertical shear induced GPI anomaly over the Central America (Fig. 5b), which dominates the GPI difference between *AtlCB* and *CTRL* (Fig. 4b).

3.2 Pacific SST biases

Unlike the Atlantic cold bias, which significantly impacts both the Atlantic and eastern Pacific basins (Fig. 2), the Pacific cold bias has no significant impact on TC track density in these ocean basins (Fig. 8). The Pacific warm bias and total bias significantly increase the track density and genesis density (not shown) locally in the ENP, but the positive anomaly pattern has a different shape and location from that of the *AtlCB* experiment. While the maximum magnitudes of the track density anomaly from *PacWB* and *PacTB* are about half of that from the Atlantic cold bias, the positive TC track density anomaly in the central Pacific (around 180°W) is much larger in *PacCB* and *PacTB* compared to *AtlCB*. A positive track density anomaly in the central North Pacific

occurs with a negative anomaly in the central to eastern Atlantic basin in both *PacCB* and *PacTB* (Fig. 8b, c). Since the positive anomaly in the central Pacific is accompanied by a negative anomaly in the western (coastal) Pacific, an eastward shift of TCs in the WNP is generated by the Pacific total SST bias (Fig. 8c).

This eastward shift also appears in genesis density (not shown), and a similar shift in WNP TCs is observed during El Niño events (e.g. Chan 1985, 2005; Wang and Chan 2002). Wang and Chan (2002) suggest that the equatorial westerlies and upper-level divergence induced by the intensified WNP subtropical high during El Niño events can both contribute to a southeastward shift of TCs, by enhancing TC generation in southeastern WNP and suppressing generation over the northwestern quadrant of the WNP. In our case, similar anomalous westerlies can be generated by the zonal SST gradient induced by the zonal pattern of cold and warm biases north of the equator, and the intensification of the subtropical high can be generated by the local decrease in SST induced by the northwestern part of the Pacific cold bias. Therefore, with both the warm and cold biases combined, *PacTB* generates the most significant eastward shift in TCs. However, the SST bias pattern in the Pacific is more complex than El Niño related SST anomalies, and further work is required to fully understand their impact on the shift of TC locations, and how the mechanism is different from that during El Niño events.

Consistent with the impact on the track density, the Pacific cold bias alone insignificantly influences ACE and the number of TCs in both the Atlantic and Pacific basins (Fig. 9; Table 3). The warm bias, on the other hand, locally

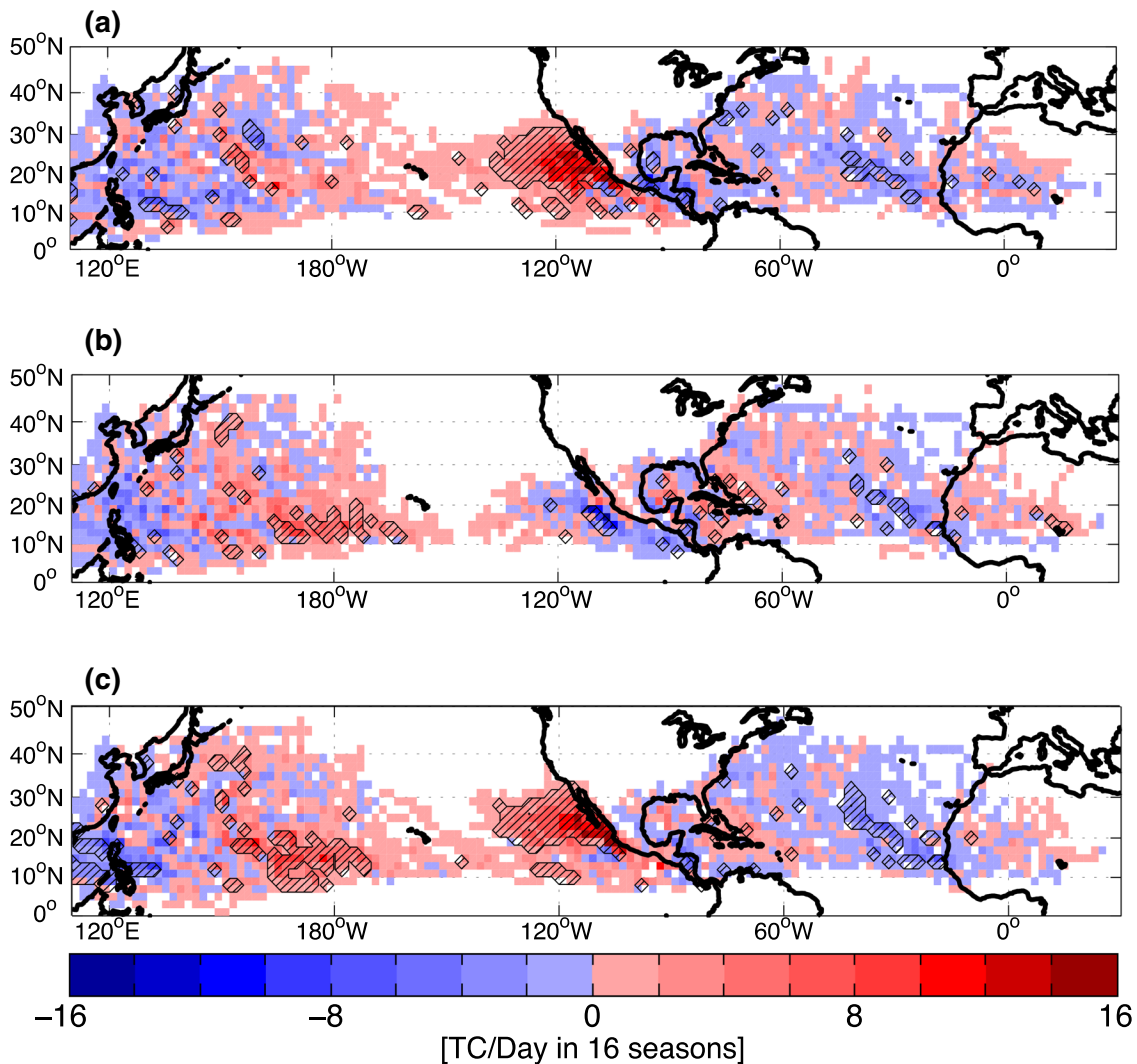


Fig. 8 The differences between track density ensemble means of **a** Pacific warm bias (*PacWB*) and control (*CTRL*) runs, **b** Pacific cold bias (*PacCB*) and control (*CTRL*) runs, and **c** Pacific total bias

(*PacTB*) and control (*CTRL*) runs. Hatched regions passed the two-sample student t-test at 5% significance level

increases ENP TC activity (Fig. 9b, e). Similarly, the ensemble-mean values of ACE and the number of TCs increase (Table 3). Furthermore, the *PacWB* runs generate stronger TCs in the ENP (not shown), consistent with the larger ACE values. The remote impact of the Pacific warm bias on TC activity in Atlantic is evident, with a slight decrease in ACE (significant) and number of TCs (insignificant) (Fig. 9a, d; Table 3). Moreover, there is no significant change in the ensemble means of both ACE and number of TCs in the Atlantic basin in *PacTB*. The ensemble means show that while the Atlantic SST biases have a larger impact on TCs remotely in the ENP compared to locally in Atlantic (Table 2), the Pacific biases have a larger impact locally in the ENP (Table 3).

Even though the Pacific SST bias has no significant impact on WNP ACE and number of TCs, the probability

density function of TC intensity (not shown) indicates that *PacCB* shifts the TCs to lower intensity compared to *CTRL*. A similar result is obtained by separating out strong TCs when calculating the ensemble-mean ACE and the number of TCs. While the ensemble-averaged values of ACE and the number of TCs in *PacCB* are insignificantly different from those in *CTRL* (Table 3), the *PacCB* ensemble mean of ACE for TCs stronger than category 3 shows a 61% decrease from *CTRL* in WNP. Besides the change in ACE, the number of TCs stronger than category 3 also decreases in *PacCB* (by 75%), indicating that a significant decrease in WNP TC intensity can be caused by the Pacific cold bias.

GPI and associated atmospheric variables are also analyzed for Pacific bias experiments to investigate the impact of Pacific SST biases on TC-related environments. Locally, *PacWB* and *PacTB* strongly increase GPI in the ENP,

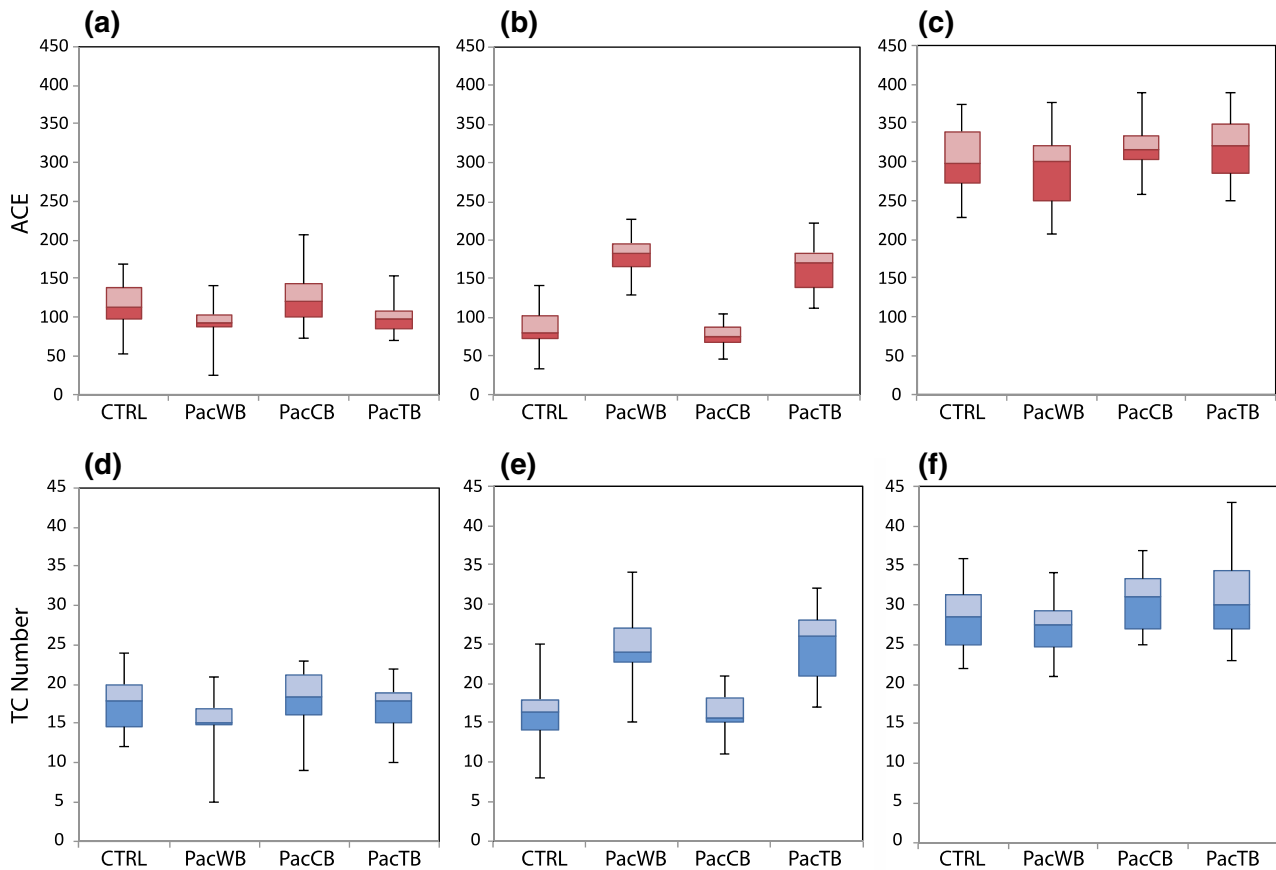


Fig. 9 Boxplot of simulated Accumulated Cyclone Energy (ACE) (a–c) and number of TCs (d–f) from control (*CTRL*), Pacific warm (*PacWB*), cold (*PacCB*), and total (*PacTB*) bias runs (16 ensemble members each) in Atlantic (a, d), eastern North Pacific (b, e), and western North Pacific (c, f) basins. The horizontal line between light

and dark shading represents the median of the ensemble values, while the upper boundary of the light color box represents the 75 percentile and the lower boundary of the dark color box represents the 25 percentile. The whiskers show the maximum and minimum ensemble values

Table 3 Ensemble means (from 16 ensemble members each) of ACE and the number of TCs from control (*CTRL*) and Pacific bias (*PacWB*, *PacCB*, and *PacTB*) runs in both real number and percentage difference from *CTRL* (only shown if the difference from *CTRL* is significant at the 5% level)

	<i>CTRL</i>	<i>PacWB</i>	<i>PacCB</i>	<i>PacTB</i>
Atlantic ACE	116	92 [– 21%]	125	100
ENP ACE	87	181 [108%]	75	166 [91%]
WNP ACE	302	292	314	317
Atlantic number of TCs	18	15	18	17
ENP number of TCs	16	25 [56%]	16	25 [56%]
WNP number of TCs	28	27	31	31

corresponding to an increase in ACE and number of TCs in that region (Fig. 10). *PacCB* remotely increases GPI in the western Atlantic near the Caribbean Sea (Fig. 10b), corresponding to an insignificant increase in ACE in Atlantic basin (Table 3). *PacTB* has the combined effect of *PacWB* and *PacCB* in the ENP and Atlantic basins, where GPI

increases strongly in the ENP, but changes insignificantly in the Atlantic. Both *PacWB* and *PacCB* (and thus *PacTB*) generate a positive GPI anomaly in the central Pacific near 10°–15°N and 160°E–150°W, and a negative anomaly north of the positive anomaly in central Pacific as well as in the WNP. Note that a similar pattern is shown in the track density anomalies for *PacTB* (Fig. 8), except for a westward shifted pattern compared to the GPI anomalies.

The contributions from different terms in GPI indicate that the warm bias generates an increase in GPI in the ENP mainly through PI (Fig. 11). *PacWB* and *PacCB* have similar GPI anomalies in the central Pacific derived from similar physical causes: both humidity and shear terms make a positive GPI anomaly. This similarity between the GPI term contributions in *PacWB* and *PacCB* suggests that it is the gradient of the SST, rather than the SST anomaly, that influences the atmospheric circulation and condition (Graham and Barnett 1987; Wang and Li 1993), which further induce changes in TC activity. Nevertheless, the negative GPI anomaly in the central Pacific and WNP is

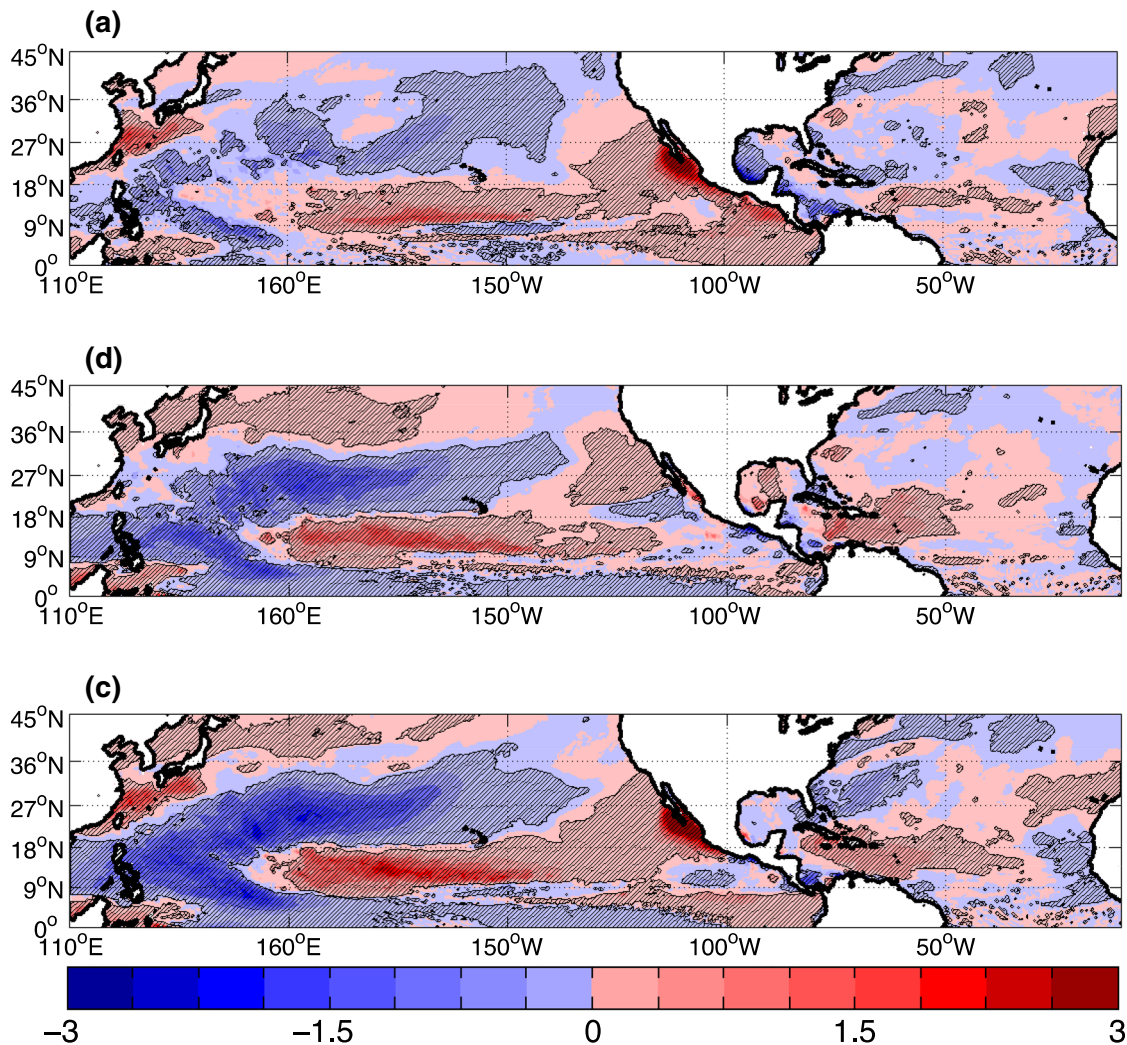


Fig. 10 The differences between GPI ensemble means of **a** Pacific warm bias (*PacWB*) and control (*CTRL*) runs, **b** Pacific cold bias (*PacCB*) and control (*CTRL*) runs, and **c** Pacific total bias (*PacTB*)

and control (*CTRL*) runs. Hatched regions passed the two-sample student t-test at 5% significance level

much weaker in *PacWB* than *PacCB*, with the anomaly attributed to all GPI terms. Although the *PacCB* generates a stronger eastward shift in the WNP TC tracks and GPI anomaly, with the cold bias in western WNP, TCs do not seem to intensify further even with a longer distance to travel over the ocean, which can potentially intensify TCs (eg. Wang and Chan 2002; Camargo and Sobel 2005; Wang et al. 2013). This could be related to the coarse resolution of the model used in this study that does not fully resolve TC dynamics. As a result, the TC activity (ACE and TC number) of strong TCs decreases in *PacCB* simulations. As for the Atlantic bias experiments, all the analyses for the Pacific SST bias experiments have been repeated by randomly chosen 8 ensemble members, and the results remain similar to those with all (16) ensemble members.

3.3 Atlantic and Pacific SST biases

Given the importance of joint SST variability (Patricola et al. 2014), we expect the Atlantic and Pacific biases to jointly influence the TC simulations. Both Atlantic total bias (*AtlTB*) and Pacific total bias (*PacTB*) generate an increase in track density in ENP (Fig. 12), with *AtlTB* from about 10°N to 20°N (Fig. 2c), and *PacTB* from about 20°N to 30°N (Fig. 8c). Note that while the strongest increase of the track density in *PacTB* is along the west coast of Central America (corresponding to the bias location), the anomaly in *AtlTB* is slightly offshore in the ENP (due to the local topographic impact). The impact of the combined Atlantic and Pacific SST biases (*AtlPacTB*) is shown to have combined effects of *AtlTB* and *PacTB* (Fig. 12). Compared to *AtlTB* and *PacTB*,

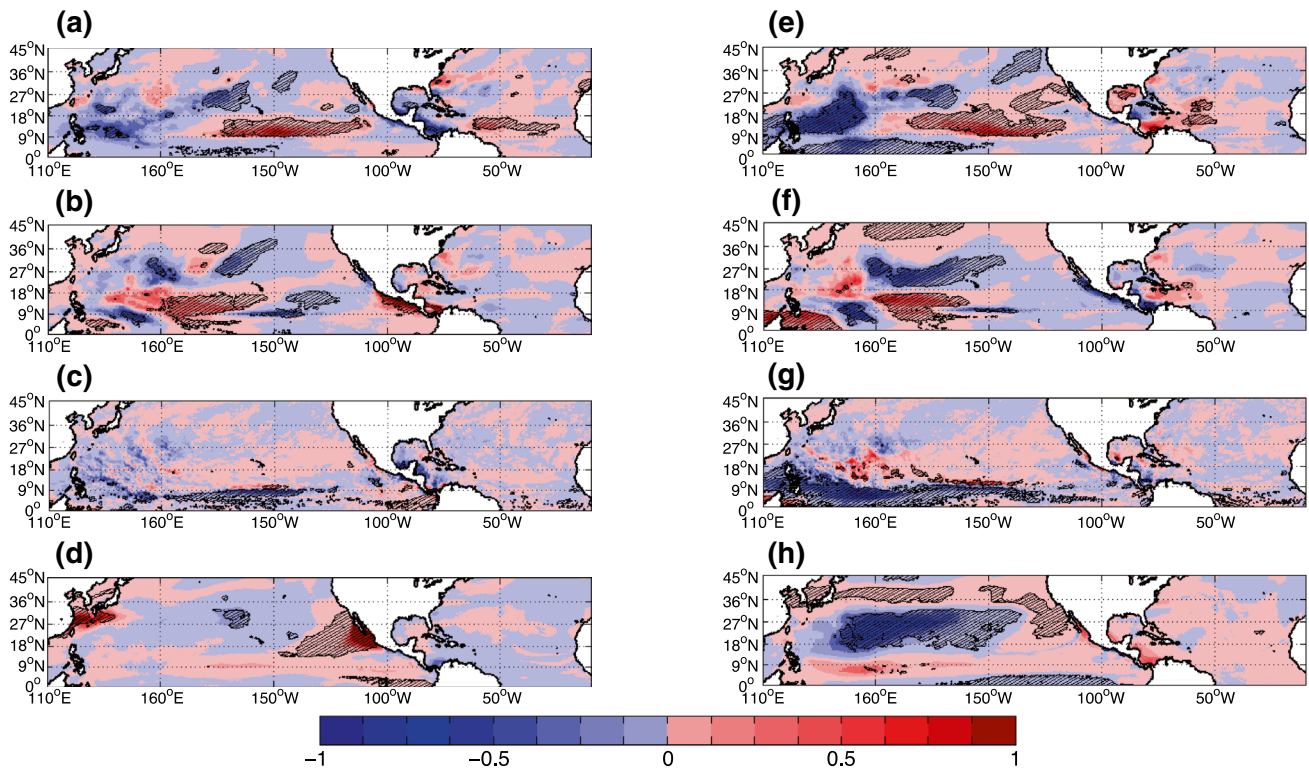


Fig. 11 The contribution on the differences of GPI ensemble means between Pacific warm (*PacWB*) bias runs and control (*CTRL*) runs from **a** humidity, **b** shear, **c** vorticity, and **d** potential intensity terms; and the contribution on the differences between Pacific cold (*PacCB*)

bias runs and control (*CTRL*) runs from **e** humidity, **f** shear, **g** vorticity, and **h** potential intensity terms. Hatched regions passed the two-sample student t-test at 5% significance level

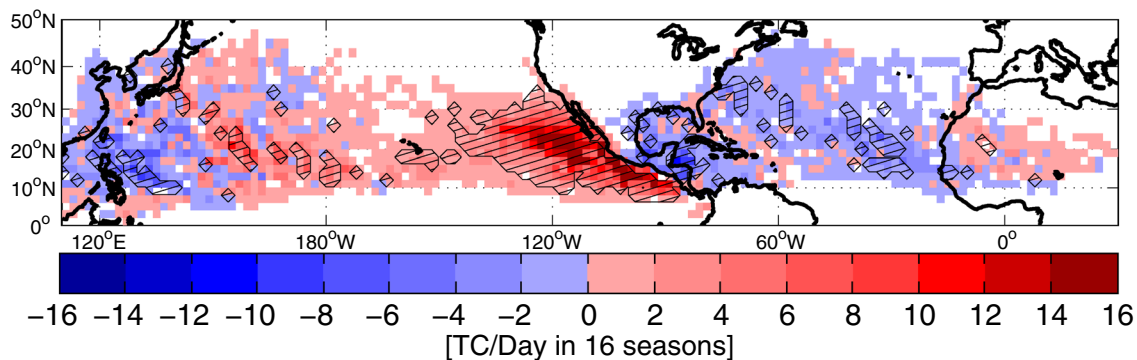


Fig. 12 The differences between track density ensemble means of Atlantic and Pacific total bias (*AtlPacTB*) runs, and that of control (*CTRL*) runs. Hatched regions passed the two-sample student t-test at 5% significance level

it is clear that the positive track density anomaly in the ENP is more widespread in *AtlPacTB*. In the Atlantic region, SST biases in both *AtlTB* and *PacTB* contribute to the negative anomalies in TC track density in *AtlPacTB*. However, the positive track density anomalies in the central Pacific and negative anomalies in the WNP appear to mainly come from the Pacific SST biases (*PacTB*), with minor contributions from the Atlantic biases (*AtlTB*).

The combined Atlantic and Pacific SST biases significantly reduce the values of ACE and TC numbers in the Atlantic basin, and this suppression of TC activity is mainly dominated by the Atlantic bias (Fig. 13; Table 4). In the ENP, both *AtlTB* and *PacTB* significantly increase the values of ACE and TC number, resulting in a significantly large increase in TC activity (199% and 88% compared to *CTRL* for ensemble-mean ACE and TC numbers, respectively)

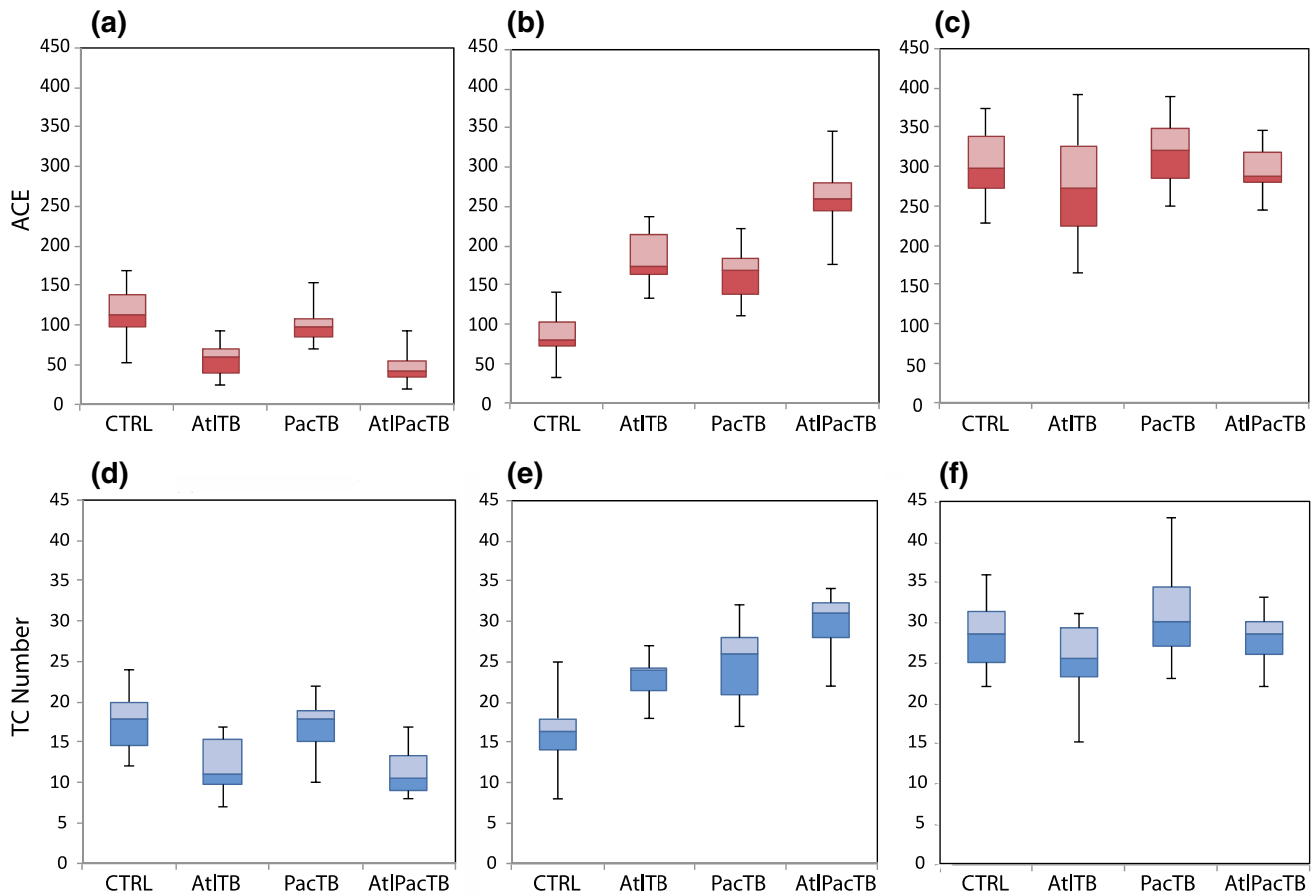


Fig. 13 Boxplot of simulated Accumulated Cyclone Energy (ACE) (a–c) and number of TCs (d–f) from control (*CTRL*), Atlantic total (*AtlTB*), Pacific total (*PacTB*), and combined Atlantic and Pacific total (*AtlPacTB*) bias runs (16 ensemble members each) in Atlantic (a, d), eastern North Pacific (b, e), and western North Pacific (c, f)

basins. The horizontal line between light and dark shading represents the median of the ensemble values, while the upper boundary of the light color box represents the 75 percentile and the lower boundary of the dark color box represents the 25 percentile. The whiskers show the maximum and minimum ensemble values

Table 4 Ensemble means (from 16 ensemble members each) of ACE and the number of TCs from control (*CTRL*), Atlantic total bias (*AtlTB*), Pacific total bias (*PacTB*), and combined Atlantic and Pacific total bias (*AtlPacTB*) runs in both real number and percentage difference from *CTRL* (only shown if the difference from *CTRL* is significant at the 5% level)

	<i>CTRL</i>	<i>AtlTB</i>	<i>PacTB</i>	<i>AtlPacTB</i>
Atlantic ACE	116	57 [– 51%]	100	47 [– 59%]
ENP ACE	87	185 [113%]	166 [91%]	260 [199%]
WNP ACE	302	278	317	297
Atlantic number of TCs	18	12 [– 33%]	17	11 [– 39%]
ENP number of TCs	16	23 [44%]	25 [56%]	30 [88%]
WNP number of TCs	28	25	31	28

in *AtlPacTB* runs. However, the ensemble-mean ACE and TC numbers show relatively minor changes in the WNP in *AtlPacTB* compared to *AtlTB* and *PacTB* (Table 4).

Interestingly, there is an indication that the ensemble spread, which is a measure of atmospheric internal variability, is reduced in WNP when the Atlantic and Pacific SST biases are combined in *AtlPacTB* compared to that in *AtlTB* and *PacTB* respectively. Whether this change in internal variability is robust requires further research.

To investigate the environmental condition changes associated with the impact of combined bias on TC simulations, we also computed GPI for the *AtlPacTB* experiment (Fig. 14). According to the GPI anomalies induced by individual Atlantic and Pacific SST biases (Figs. 4, 10, respectively), the negative GPI anomalies in Atlantic basin in *AtlPacTB* are mainly driven by the Atlantic cold bias, whereas the positive GPI anomalies in the ENP are caused by joint impacts from the Atlantic cold bias and Pacific warm bias. In the central Pacific and WNP region, the GPI anomaly in *AtlPacTB* shows a similar pattern and magnitude to the Pacific bias experiments, indicating the dominant influence is from the Pacific biases, rather than the Atlantic biases, on the

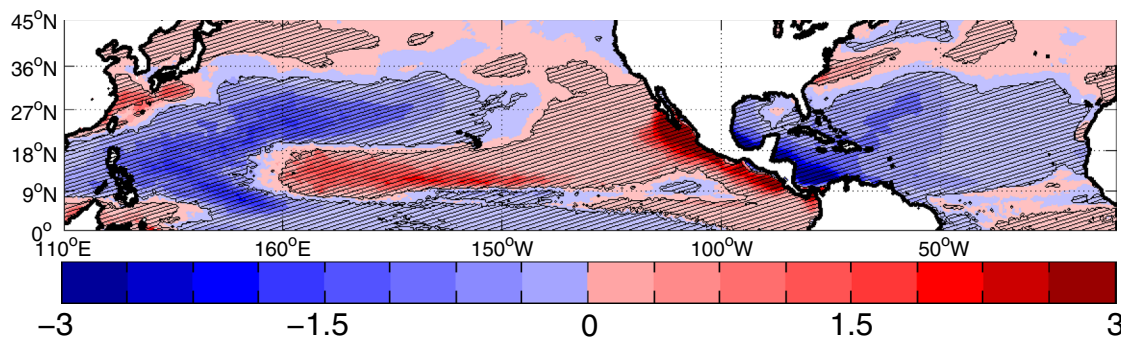


Fig. 14 The differences between GPI ensemble means of combined Atlantic and Pacific bias (*AtlPacTB*) runs and that of control (*CTRL*) runs

GPI in these regions. This GPI anomaly pattern is generally consistent with TC changes measured by other TC activity indexes, including track density, ACE, and number of TCs. It shows that TC activity is (1) strongly enhanced in the ENP, (2) suppressed in the Atlantic, and (3) generally increased in the central Pacific and decreased in the WNP because of an eastward shift in TC locations, under the combined influence of SST biases in both basins.

4 Discussion and summary

Large ensembles of TC-permitting tropical-channel WRF simulations show that tropical SST biases common to current generation climate models can have a significant impact on TC simulations, predictions, and projections both locally in and remotely from tropical Atlantic and Pacific basins. Even though previous studies have suggested impacts of SST biases on simulated TCs (Vecchi et al. 2014), the influence of individual biases (and biases in each basin) has not been systematically investigated. In this study, we investigate the local and remote TC responses to individual biases by separating warm and cold biases in each ocean basins, and the results allow us to identify which biases have the most significant impact on TC simulations. Our study shows that tropical SST biases can cause an overestimation of ACE (by ~200%) in the ENP and underestimation of ACE (by ~60%) in Atlantic, while the impact on WNP ACE is insubstantial. Considering the basin-wide TC activity, TCs in the ENP appear to be most affected by SST biases because of the joint influence from the tropical Atlantic and Pacific. In contrast, Atlantic TC activity is mostly affected by the cold bias in the Northern Tropical Atlantic, whereas TC activity in the WNP seems to be dominated by the local influence of Pacific SST biases.

Some previous TC studies based on CMIP5 multi-model simulations also indicate the possible impact of the SST biases on the simulated TC activity. For example, with comparable model resolutions, Tory et al. (2013) show

significant differences among simulated TC activity by different models, and suggest factors other than the resolution may play a key role in generating the simulated TC activity biases. Camargo (2013) suggests the potential contribution of SST biases to the TC biases in models, especially in the North Atlantic region. For instance, some models show relatively low TC number in the North Atlantic and unrealistically high TC activity in the ENP with negative SST biases in the Atlantic, which is consistent with our finding from the bias-included simulations. They point out the marginal nature of the North Atlantic environments for TC formations, and suggest even small negative SST biases can lead to a suppression of simulated TC activity in the region. Reed et al. (2015) also indicate SST with problematic drift can significantly influence the TC activity downscaled from global model simulations. Therefore, with the support from previous studies, the results of our study suggest that reducing the Atlantic cold SST bias and Pacific SST warm biases could potentially have the impact of improving TC representation in climate simulations, especially in the ENP and Atlantic. Moreover, even though the spatial patterns and magnitudes are similar between the Atlantic and Pacific SST biases, the mechanisms of how these biases exert their influence on simulated TC activity are different.

The Atlantic cold SST bias causes decreases in mid-tropospheric humidity and potential intensity, and increases in vertical wind shear, all of which contribute to decreases in the North Tropical Atlantic GPI, leading to decreases in track density, ACE, and number of TCs in the region. In addition, increases in ENP GPI (together with increases in track density, ACE, and TC numbers) primarily come from decreases in vertical wind shear due to the remote influence of the Atlantic cold SST bias that produces a Walker-type response (Patricola et al. 2017) forced by a diabatic heating anomaly associated with orographic lifting along Central American mountain ranges. The terrain-induced circulation anomaly enhances vertical wind shear over the Atlantic sector and reduces vertical wind shear in the near coast region of ENP. Figure 15 shows a schematic diagram

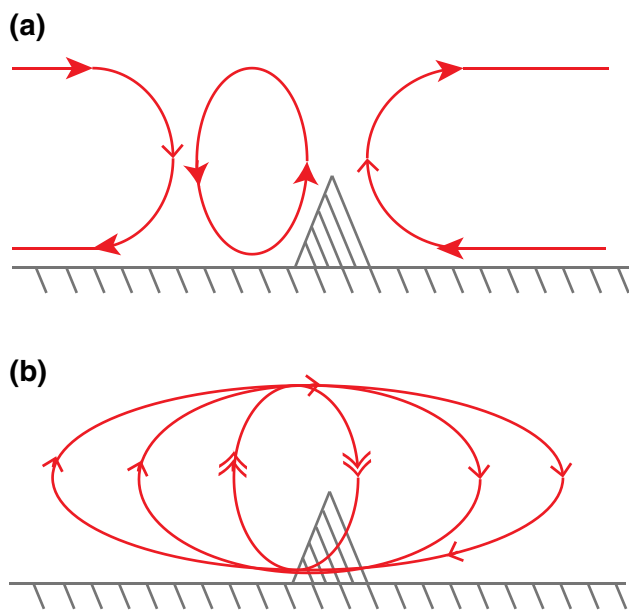


Fig. 15 The mechanism of remote influence of the Atlantic cold bias (*AtlCB*) on ENP TCs. **a** Shows the *CTRL* circulation pattern, and **b** shows the anomalous circulation between *AtlCB* and *CTRL* runs

illustrating the mechanism behind the anomalous circulation. In response to the cold bias in Atlantic (*AtlCB*), the CLLJ intensifies because of the increase in both inter-basin SST gradient and land-sea temperature contrast. At the same time, atmospheric moisture content also decreases due to the surface cooling, which is the strongest in the Southern Caribbean (Fig. 1). The drier and colder winds carried by the CJLJ reduces the orographic lifting induced diabatic heating, which in turn produces a clockwise anomalous vertical circulation over Central America (Fig. 15b). The anomalous circulation acting on the mean circulation (Fig. 15a) produces intensified vertical wind shear on the Atlantic side and reduced shear on the Pacific side of Central America, which is primarily responsible for the enhanced TC activity over the ENP and reduced TC activity over the Caribbean and Atlantic in *AtlBC*. This remote influence of Atlantic SST is supported by observational analysis that shows an increase in ENP TCs during cold AMM phase (Patricola et al. 2017). Both observations and simulations from the TCM show a decrease in vertical wind shear in ENP during negative AMM events. Furthermore, even though the impact of Atlantic SST biases on WNP TCs is insubstantial, Yu et al. (2015) noted a possibility of the influence of Atlantic SST variability on the circulation in Pacific Ocean. Therefore, accurate simulations of Pacific TCs will require a realistic representation of Atlantic SST.

The spatial distribution of the SST biases and the known influence of tropical SST on TCs (e.g., Vimont and Kossin 2007; Patricola et al. 2014, 2017) together suggest that the

Atlantic SST biases, which have a similar spatial structure to the negative phase of AMM, is a leading cause for failure of climate models to accurately simulate Atlantic and ENP TC activities. On the other hand, the impact of the equatorial Pacific biases is more complex than ENSO's impact on TCs because the SST biases have a more complex spatial structure along the equator than ENSO SST anomalies. The SST bias in the northwestern Pacific has a similar pattern to its counterpart in the north tropical Atlantic, but its impact on TCs is different from the Atlantic because, unlike the Atlantic, SST anomalies in the WNP have a limited influence on western Pacific TCs [Chan 2005], suggesting that dynamic processes controlling SSTs' influence on TCs are different between these two regions. We further note that the net effect of the Atlantic and Pacific biases on TCs simulated by AtlPacTB cannot be simply deduced by linear superposition of the effects from *AtlTB* and from *PacTB*, although some compensation between the effects of different SST biases on TC activity is observed. This suggests that the impact of the SST biases on TCs are inherent nonlinear.

In contrast to Atlantic SST biases, the Pacific SST biases do not exhibit as strong a remote influence on Atlantic TCs as the Atlantic biases do on Pacific TCs. The warm SST bias off the west coast of Mexico has a significant impact on ENP TCs, which is mainly driven by local change in potential intensity (which is further a function of SST). Moreover, anomalies in the WNP suggest an eastward shift of the TCs due to the Pacific SST biases, possibly through a mechanism similar to the southeastward shift of WNP TCs that attributes to El Niño events (Wang and Chan 2002). While our results show no significant impact of Pacific SST on Atlantic TCs, previous studies have shown a remote influence of ENSO variability on the TC activity in the Atlantic basin. Given that the regions with larger SST biases in the Pacific basin are not in the El Niño regions, it suggests that the location of the maximum SST anomalies (or biases) may play an important role controlling the impact on TCs, as suggesting by Wang and Chan (2002). However, further research is required to reach a conclusion.

Our results suggest that SST biases can change TC tracks, and thus TC landfall locations. In other words, tropical SST biases can introduce biases to our forecast of regional TC landfall. For example, the Pacific biases introduce an eastward shift in the WNP TC tracks, suggesting a reduced possibility of TC landfall in the Asian region. Therefore, projections of future TC changes over the Asian region, particularly TC landfall over East Asia, may be subject to considerable uncertainties because of SST biases in coupled models. A similar shift in WNP TC tracks is shown in Fig. 1 in Vecchi et al. (2014). By removing the SST biases through flux adjustment, the WNP TCs are generated more toward the Asian region and less in the Central Pacific region. Moreover, both our result and that from Vecchi

et al. (2014) suggest an increase in track and genesis of TCs in near-coastal region of the ENP in the presence of SST biases, indicating a possible overestimation of Northern and Central American TC landfall from the Pacific Ocean. Nevertheless, while our simulations with Atlantic biases show a basin-wide decrease in TC tracks, indicating no significant change in the TC locations, Vecchi et al. (2014) show a southeastward shifted in tracks and genesis locations, suggesting a reduced probability of TCs making landfall over US and Mexico from the GoM and western Atlantic Ocean. We should note that Vecchi et al. (2014) consider the SST biases not only in the tropic, but also in extratropics, and the sample size in their simulations is about twice of our TCM simulations.

Even though our ensemble size is shown to be sufficient for computing basin-wide TC activities, it is possible that our sample size is not large enough to thoroughly investigate systematic shifts in the Atlantic TC tracks and genesis locations caused by SST biases. Moreover, we utilized a TC-permitting atmospheric-only model, while Vecchi et al. (2014) utilized a high-resolution atmospheric model coupled to a low-resolution ocean model. Due to the differences in experimental designs between this study and Vecchi et al. (2014), it is difficult to directly compare the results. Furthermore, while our results suggest the importance of the response in the Caribbean and western north Atlantic, the model we utilized (TCM) is known to have convection biases in these regions. Therefore, an oversensitivity of TC responses may be present in our TCM. However, this problem of regional convection biases is also a general problem among many AGCMs (Biasutti et al. 2006). One should keep these convection biases in mind when interpreting our results.

In conclusion, our results suggest the SST biases can influence simulations, seasonal forecasts, and future projections of TCs not only in local basins, but also in remote ocean basins. Therefore, we should take the SST biases and their impact into account when analyzing TC projections from coupled AOGCMs. We note that the magnitude of the SST biases in individual models may be more or less severe than that from the multi-model ensemble bias used in this study, suggesting that the impacts of the SST biases on TC simulations can vary from model to model. Many previous studies focus on the origins of these SST biases (Richter and Xie 2008; Li and Xie 2012; Patricola et al. 2012; Xu et al. 2014b; Small et al. 2015), and some progress has been made to improve the SST biases, even though the improvement has shown to be difficult and challenging in some specific regions such as the eastern ocean basins (Xu et al. 2014a, b; Richter 2015; Small et al. 2015; Zuidema et al. 2016). Nevertheless, the bias problem is unlikely to be resolved in the near future and the climate modeling community will continue to confront this problem (Richter 2015). Moreover, since tropical SST biases can have remote effects on

biases in other regions, it could potentially hinder the effort to improve regional processes to address local SST biases, making the reduction of SST biases more challenging (Wang et al. 2014). This means that we need to develop strategies of coping with the impact of these model biases at least in the near future. With only few studies focusing on the impact of SST biases on TC simulations and predictions, more investigations are needed to have a comprehensive understanding of local and remote influence of the SST biases on TC simulations on seasonal to decadal timescales.

Acknowledgements The authors wish to thank the editor and two anonymous reviewers for comments that greatly improved the quality of this paper. This research is supported by U.S. National Science Foundation Grants OCE-1334707, AGS-1347808 and AGS-1462127, and National Oceanic and Atmospheric Administration Grant NA13OAR4310136. PC acknowledges the Natural Science Foundation of China (41490644 and 41490640). C.M.P. acknowledges support from the U.S. Department of Energy, Office of Science, Office of Biological and Environmental Research, Climate and Environmental Sciences Division, Regional & Global Climate Modeling Program, under Award Number DE-AC02-05CH11231. High-performance computing resources provided by the Extreme Science and Engineering Discovery Environment (XSEDE). Simulations were performed at the Texas Advanced Computing Center (TACC) at the University of Texas at Austin and the Texas A&M Supercomputing Facility.

References

- Bell GD, Halpert MS, Schnell RC et al (2000) Climate assessment for 1999. *Bull Am Meteorol Soc* 81:s1–s50. [https://doi.org/10.1175/1520-0477\(2000\)81%5BS1:CAF%5D2.0.CO;2](https://doi.org/10.1175/1520-0477(2000)81%5BS1:CAF%5D2.0.CO;2)
- Bender MA, Knutson TR, Tuleya RE et al (2010) Modeled impact of anthropogenic warming on the frequency of intense Atlantic hurricanes. *Science* 327:454–458. <https://doi.org/10.1126/science.1180568>
- Biasutti M, Sobel AH, Kushnir Y (2006) AGCM precipitation biases in the tropical Atlantic. *J Clim* 19:935–958. <https://doi.org/10.1175/JCLI3673.1>
- Blake ES, Rappaport EN, Jarrell JD et al (2007) The deadliest, costliest, and most intense United States tropical cyclones from 1851 to 2006 (and other frequently requested hurricane facts). NOAA/National Weather Service, National Centers for Environmental Prediction, National Hurricane Center Miami
- Blake ES, Kimberlain TB, Berg RJ et al (2013) Tropical cyclone report hurricane Sandy. National Hurricane Center 12: 1–10
- Camargo SJ (2013) Global and regional aspects of tropical cyclone activity in the CMIP5 models. *J Clim* 26:9880–9902. <https://doi.org/10.1175/JCLI-D-12-00549.1>
- Camargo SJ, Hsiang SM (2016) From the influence of climate to their socioeconomic impacts. In: *Tropical cyclones*, pp 303–342
- Camargo SJ, Sobel AH (2005) Western North Pacific tropical cyclone intensity and ENSO. *J Clim* 18:2996–3006. <https://doi.org/10.1175/JCLI3457.1>
- Camargo SJ, Emanuel KA, Sobel AH (2007) Use of a genesis potential index to diagnose ENSO effects on tropical cyclone genesis. *J Clim* 20:4819–4834. <https://doi.org/10.1175/JCLI4282.1>
- Chan JCL (1985) Tropical cyclone activity in the Northwest Pacific in relation to the El Niño/Southern Oscillation phenomenon. *Mon Weather Rev* 113:599–606. [https://doi.org/10.1175/1520-0493\(1985\)113%3C0599:TCAITN%3E2.0.CO;2](https://doi.org/10.1175/1520-0493(1985)113%3C0599:TCAITN%3E2.0.CO;2)

- Chan JCL (2005) Interannual and interdecadal variations of tropical cyclone activity over the western North Pacific. *Meteorol Atmos Phys* 89:143–152. <https://doi.org/10.1007/s00703-005-0126-y>
- Colas F, McWilliams JC, Capet X, Kurian J (2012) Heat balance and eddies in the Peru–Chile current system. *Clim Dyn* 39:509–529. <https://doi.org/10.1007/s00382-011-1170-6>
- Ding H, Keenlyside NS, Latif M (2012) Impact of the equatorial Atlantic on the El Niño Southern Oscillation. *Clim Dyn* 38:1965–1972. <https://doi.org/10.1007/s00382-011-1097-y>
- Emanuel KA (2005) Increasing destructiveness of tropical cyclones over the past 30 years. *Nature* 436:686–688. <https://doi.org/10.1038/nature03906>
- Emanuel KA (2007) Environmental factors affecting tropical cyclone power dissipation. *J Clim* 20:5497–5509. <https://doi.org/10.1175/2007JCLI1571.1>
- Emanuel KA (2017) Assessing the present and future probability of Hurricane Harvey’s rainfall. *Proc Natl Acad Sci* 114:12681–12684. <https://doi.org/10.1073/pnas.1716222114>
- Emanuel KA, Nolan DS (2004) Tropical cyclone activity and the global climate system. In: 26th conference on hurricanes and tropical meteorology. American Meteorological Society, Miami, FL
- Graham NE, Barnett TP (1987) Sea surface temperature, surface wind divergence, and convection over tropical oceans. *Science* 238:657–659. <https://doi.org/10.1126/science.238.4827.657>
- Gray WM (1984a) Atlantic seasonal hurricane frequency. Part II: forecasting its variability. *Mon Weather Rev* 112:1669–1683. [https://doi.org/10.1175/1520-0493\(1984\)112%3C1669:ASHFPI%3E2.0.CO;2](https://doi.org/10.1175/1520-0493(1984)112%3C1669:ASHFPI%3E2.0.CO;2)
- Gray WM (1984b) Atlantic seasonal hurricane frequency. Part I: El Niño and 30 mb Quasi-Biennial Oscillation influences. *Mon Weather Rev* 112:1649–1668. [https://doi.org/10.1175/1520-0493\(1984\)112%3C1649:ASHFPI%3E2.0.CO;2](https://doi.org/10.1175/1520-0493(1984)112%3C1649:ASHFPI%3E2.0.CO;2)
- Ham Y-G, Kug J-S, Park J-Y (2013a) Two distinct roles of Atlantic SSTs in ENSO variability: North tropical Atlantic SST and Atlantic Niño. *Geophys Res Lett* 40:4012–4017. <https://doi.org/10.1002/grl.50729>
- Ham Y-G, Kug J-S, Park J-Y, Jin F-F (2013b) Sea surface temperature in the north tropical Atlantic as a trigger for El Niño/Southern Oscillation events. *Nat Geosci* 6:112–116. <https://doi.org/10.1038/ngeo1686>
- Holland GJ, Webster PJ (2007) Heightened tropical cyclone activity in the North Atlantic: natural variability or climate trend? *Philos Trans R Soc A Math Phys Eng Sci* 365:2695–2716. <https://doi.org/10.1098/rsta.2007.2083>
- Jien JY, Gough WA, Butler K (2015) The influence of El Niño–Southern Oscillation on tropical cyclone activity in the eastern North Pacific basin. *J Clim* 28:2459–2474. <https://doi.org/10.1175/JCLI-D-14-00248.1>
- Jin F-F, Boucharel J, Lin I-I (2014) Eastern Pacific tropical cyclones intensified by El Niño delivery of subsurface ocean heat. *Nature* 516:82–85. <https://doi.org/10.1038/nature13958>
- Kanamitsu M, Ebisuzaki W, Woollen J et al (2002) NCEP–DOE AMIP-II Reanalysis (R-2). *Bull Am Meteorol Soc* 83:1631–1644. <https://doi.org/10.1175/BAMS-83-11-1631>
- Klotzbach PJ, Bowen SG, Pielke R, Bell M (2018) Continental United States hurricane landfall frequency and associated damage: observations and future risks. *Bull Am Meteorol Soc BAMS-D-17-0184.1*. <https://doi.org/10.1175/BAMS-D-17-0184.1>
- Knutson T, Landsea C, Emanuel K (2010) Tropical cyclones and climate change: a review. In: Chan JCL, Kepert J (eds) *Global perspectives on tropical cyclones*. World Scientific, Singapore, pp 243–286
- Kucharski F, Parvin A, Rodriguez-Fonseca B et al (2016) The teleconnection of the tropical Atlantic to Indo-Pacific sea surface temperatures on inter-annual to centennial time scales: A review of recent findings. *Atmosphere (Basel)* 7:29. <https://doi.org/10.3390/atmos702029>
- LaRow TE, Stefanova L, Shin D-W, Cocks S (2010) Seasonal Atlantic tropical cyclone hindcasting/forecasting using two sea surface temperature datasets. *Geophys Res Lett* 37:L02804. <https://doi.org/10.1029/2009GL041459>
- Li G, Xie S-P (2012) Origins of tropical-wide SST biases in CMIP multi-model ensembles. *Geophys Res Lett* 39:L22703. <https://doi.org/10.1029/2012GL053777>
- Lin I-I, Black P, Price JF et al (2013) An ocean coupling potential intensity index for tropical cyclones. *Geophys Res Lett* 40:1878–1882. <https://doi.org/10.1002/grl.50091>
- Liu H, Wang C, Lee S-K, Enfield D (2012) Atlantic warm-pool variability in the IPCC AR4 CGCM simulations. *J Clim* 25:5612–5628. <https://doi.org/10.1175/JCLI-D-11-00376.1>
- Masunaga H, Nakajima TY, Nakajima T et al (2002) Physical properties of maritime low clouds as retrieved by combined use of tropical rainfall measuring mission (TRMM) microwave imager and visible/infrared scanner 2. *Climatology of warm clouds and rain*. *J Geophys Res* 107:4367. <https://doi.org/10.1029/2001JD001269>
- Murakami H, Vecchi GA, Villarini G et al (2016) Seasonal forecasts of major hurricanes and landfalling tropical cyclones using a high-resolution GFDL coupled climate model. *J Clim* 29:7977–7989. <https://doi.org/10.1175/JCLI-D-16-0233.1>
- Nobre P, Shukla J (1996) Variations of sea surface temperature, wind stress, and rainfall over the tropical Atlantic and South America. *J Clim* 9:2464–2479. [https://doi.org/10.1175/1520-0442\(1996\)009<2464:VOSSTW>2.0.CO;2](https://doi.org/10.1175/1520-0442(1996)009<2464:VOSSTW>2.0.CO;2)
- Painemal D, Minnis P (2012) On the dependence of albedo on cloud microphysics over marine stratocumulus clouds regimes determined from Clouds and the Earth’s Radiant Energy System (CERES) data. *J Geophys Res Atmos* 117:D06203. <https://doi.org/10.1029/2011JD017120>
- Patricola CM, Li M, Xu Z et al (2012) An investigation of tropical Atlantic bias in a high-resolution coupled regional climate model. *Clim Dyn* 39:2443–2463. <https://doi.org/10.1007/s00382-012-1320-5>
- Patricola CM, Saravanan R, Chang P (2014) The impact of the El Niño–Southern Oscillation and Atlantic Meridional Mode on seasonal Atlantic tropical cyclone activity. *J Clim* 27:5311–5328. <https://doi.org/10.1175/JCLI-D-13-00687.1>
- Patricola CM, Chang P, Saravanan R (2016) Degree of simulated suppression of Atlantic tropical cyclones modulated by flavour of El Niño. *Nat Geosci* 9:155–160. <https://doi.org/10.1038/ngeo2624>
- Patricola CM, Saravanan R, Chang P (2017) A teleconnection between Atlantic sea surface temperature and eastern and central North Pacific tropical cyclones. *Geophys Res Lett* 44:1167–1174. <https://doi.org/10.1002/2016GL071965>
- Polo I, Martin-Rey M, Rodriguez-Fonseca B et al (2015) Processes in the Pacific La Niña onset triggered by the Atlantic Niño. *Clim Dyn* 44:115–131. <https://doi.org/10.1007/s00382-014-2354-7>
- Rayner NA, Parker DE, Horton EB et al (2003) Global analyses of sea surface temperature, sea ice, and night marine air temperature since the late nineteenth century. *J Geophys Res* 108:4407. <https://doi.org/10.1029/2002JD002670>
- Reed A, Mann M, Emanuel K, Tittle D (2015) An analysis of long-term relationships among count statistics and metrics of synthetic tropical cyclones downscaled from CMIP5 models. *J Geophys Res Atmos* 120:7506–7519. <https://doi.org/10.1002/2015JD023357>
- Reynolds RW, Smith TM, Liu C et al (2007) Daily high-resolution-blended analyses for sea surface temperature. *J Clim* 20:5473–5496. <https://doi.org/10.1175/2007JCLI1824.1>
- Richter I (2015) Climate model biases in the eastern tropical oceans: causes, impacts and ways forward. *Wiley Interdiscip Rev Clim Chang* 6:345–358. <https://doi.org/10.1002/wcc.338>

- Richter I, Xie S-P (2008) On the origin of equatorial Atlantic biases in coupled general circulation models. *Clim Dyn* 31:587–598. <https://doi.org/10.1007/s00382-008-0364-z>
- Rodríguez-Fonseca B, Polo I, García-Serrano J et al (2009) Are Atlantic Niños enhancing Pacific ENSO events in recent decades? *Geophys Res Lett* 36:L20705. <https://doi.org/10.1029/2009GL040048>
- Shuckburgh E, Mitchell D, Stott P (2017) Hurricanes Harvey, Irma and Maria: how natural were these ‘natural disasters’? *Weather* 72:353–354. <https://doi.org/10.1002/wea.3190>
- Skamarock WC, Klemp JB, Dudhia J et al (2008) A description of the advanced research WRF version 3NCAR/TN–475+STR. <https://doi.org/10.5065/D68S4MVH>
- Small RJ, Curchitser E, Hedstrom K et al (2015) The Benguela upwelling system: quantifying the sensitivity to resolution and coastal wind representation in a global climate model. *J Clim* 28:9409–9432. <https://doi.org/10.1175/JCLI-D-15-0192.1>
- Taylor KE, Stouffer RJ, Meehl GA (2012) An overview of CMIP5 and the experiment design. *Bull Am Meteorol Soc* 93:485–498. <https://doi.org/10.1175/BAMS-D-11-00094.1>
- Toniazzo T, Mechoso CR, Shaffrey LC, Slingo JM (2010) Upper-ocean heat budget and ocean eddy transport in the south-east Pacific in a high-resolution coupled model. *Clim Dyn* 35:1309–1329. <https://doi.org/10.1007/s00382-009-0703-8>
- Tory KJ, Chand S, McBride J, Ye H, Dare R (2013) Projected changes in Late-twenty-first-century tropical cyclone frequency in 13 coupled climate models from phase 5 of the coupled model intercomparison project. *J Clim* 26:9946–9959. <https://doi.org/10.1175/JCLI-D-13-00010.1>
- Vecchi GA, Delworth T, Gudgel R et al (2014) On the seasonal forecasting of regional tropical cyclone activity. *J Clim* 27:7994–8016. <https://doi.org/10.1175/JCLI-D-14-00158.1>
- Vimont DJ, Kossin JP (2007) The Atlantic meridional mode and hurricane activity. *Geophys Res Lett* 34:L07709. <https://doi.org/10.1029/2007GL029683>
- Walsh K (1997) Objective detection of tropical cyclones in high-resolution analyses. *Mon Weather Rev* 125:1767–1779. [https://doi.org/10.1175/1520-0493\(1997\)125%3C1767:ODOTC%3E2.0.CO;2](https://doi.org/10.1175/1520-0493(1997)125%3C1767:ODOTC%3E2.0.CO;2)
- Wang B, Chan JCL (2002) How strong ENSO events affect tropical storm activity over the western North Pacific. *J Clim* 15:1643–1658. [https://doi.org/10.1175/1520-0442\(2002\)015%3C1643:HSEEAT%3E2.0.CO;2](https://doi.org/10.1175/1520-0442(2002)015%3C1643:HSEEAT%3E2.0.CO;2)
- Wang C, Lee S-K (2009) Co-variability of tropical cyclones in the North Atlantic and the eastern North Pacific. *Geophys Res Lett* 36:L24702. <https://doi.org/10.1029/2009GL041469>
- Wang B, Li T (1993) A simple tropical atmosphere model of relevance to short-term climate variations. *J Atmos Sci* 50:260–284. [https://doi.org/10.1175/1520-0469\(1993\)050%3C0260:ASTAM%3E2.0.CO;2](https://doi.org/10.1175/1520-0469(1993)050%3C0260:ASTAM%3E2.0.CO;2)
- Wang C, Li C, Mu M, Duan W (2013) Seasonal modulations of different impacts of two types of ENSO events on tropical cyclone activity in the western North Pacific. *Clim Dyn* 40:2887–2902. <https://doi.org/10.1007/s00382-012-1434-9>
- Wang C, Zhang L, Lee S-K et al (2014) A global perspective on CMIP5 climate model biases. *Nat Clim Chang* 4:201–205. <https://doi.org/10.1038/nclimate2118>
- Webster PJ, Holland GJ, Curry JA, Chang H-R (2005) Changes in tropical cyclone number, duration, and intensity in a warming environment. *Science* 309:1844–1846. <https://doi.org/10.1126/science.1116448>
- Whitney LD, Hobgood JS (1997) The relationship between sea surface temperatures and maximum intensities of tropical cyclones in the eastern North Pacific ocean. *J Clim* 10:2921–2930. [https://doi.org/10.1175/1520-0442\(1997\)010%3C2921:TRBSS%3E2.0.CO;2](https://doi.org/10.1175/1520-0442(1997)010%3C2921:TRBSS%3E2.0.CO;2)
- Whyte FS, Taylor MA, Stephenson TS, Campbell JD (2008) Features of the Caribbean low level jet. *Int J Climatol* 28:119–128. <https://doi.org/10.1002/joc.1510>
- Xu Z, Chang P, Richter I et al (2014a) Diagnosing southeast tropical Atlantic SST and ocean circulation biases in the CMIP5 ensemble. *Clim Dyn* 43:3123–3145. <https://doi.org/10.1007/s00382-014-2247-9>
- Xu Z, Li M, Patricola CM, Chang P (2014b) Oceanic origin of south-east tropical Atlantic biases. *Clim Dyn* 43:2915–2930. <https://doi.org/10.1007/s00382-013-1901-y>
- Yu J-Y, Kao P, Paek H et al (2015) Linking emergence of the Central Pacific El Niño to the Atlantic Multidecadal Oscillation. *J Clim* 28:651–662. <https://doi.org/10.1175/JCLI-D-14-00347.1>
- Zhang L, Wang C, Song Z, Lee S-K (2014) Remote effect of the model cold bias in the tropical North Atlantic on the warm bias in the tropical southeastern Pacific. *J Adv Model Earth Syst* 6:1016–1026. <https://doi.org/10.1002/2014MS000338>
- Zhang W, Vecchi GA, Villarini G et al (2017) Modulation of western North Pacific tropical cyclone activity by the Atlantic Meridional Mode. *Clim Dyn* 48:631–647. <https://doi.org/10.1007/s00382-016-3099-2>
- Zhao M, Held IM, Vecchi GA (2010) Retrospective forecasts of the hurricane season using a global atmospheric model assuming persistence of SST anomalies. *Mon Weather Rev* 138:3858–3868. <https://doi.org/10.1175/2010MWR3366.1>
- Zuidema P, Chang P, Medeiros B et al (2016) Challenges and prospects for reducing coupled climate model SST biases in the eastern tropical Atlantic and Pacific Oceans: The U.S. CLIVAR eastern tropical oceans synthesis working group. *Bull Am Meteorol Soc* 97:2305–2328. <https://doi.org/10.1175/BAMS-D-15-00274.1>
- Landsea CW, Franklin JL, Beven JL (2015) The revised Atlantic hurricane database (HURDAT2). United States National Oceanic and Atmospheric Administration’s National Weather Service

Publisher’s Note Springer Nature remains neutral with regard to jurisdictional claims in published maps and institutional affiliations.